X-RAY DIFFRACTION STUDIES ON LAMELLAR STRUCTURES OF LIPID BILAYERS AND OF LIPID - PROTEIN COMPLEXES

YŌJI INOKO

Department of Biophysical Engineering,

Faculty of Engineering Science,

Osaka University

March 1978

TABLE OF CONTENTS

ABSTRACT

This thesis presents results of X-ray diffraction studies of lipid-protein-water systems, which provide basic information on the interactions between lipid bilayers (Chapter I), between lipid bilayer and water (Chapter II) and between lipid bilayer and protein molecules (Chapter III). These interactions should exist in biological systems and also seem to be important concerning coacervation.

Chapter I. Effects of Cations on Dipalmitoyl Phosphatidylcholine - Cholesterol - Water Systems

X-ray diffraction studies have been made on the effects of cations upon the dipalmitoyl phosphatidylcholine-water system, which originally consists of a lamellar phase with period of 64.5 Å and of excess water. Addition of 1 mM $CaCl_2$ destroys the lamellar structure and makes it swell into the excess water. The lamellar phase, however, reappears when the concentration of $CaCl_2$ increases: a partially disordered lamellar phase with the repeat distance of 150 ∿ 200 Å comes out at the concentration of about 10 mM, the lamellar diffraction lines become sharp and the repeat distance decreases with increasing $CaCl_2$ concentration. $MgCl_2$ induces the lamellar phase of large repeat distance, whereas LiCl,

NaCl, KCl, $SrCl_2$ and $BaCl_2$ exhibit practically no effect by themselves. Incorporation of cholesterol into the phosphatidylcholine bilayers tends to stabilize the lamellar phase.

The high-angle reflections indicate that molecular arrangements in phosphatidylcholine bilayers change at $CaCl_2$ concentrations around 0.5 M. The bilayers at high $CaCl_2$ concentration seem to consist of two phases of pure phosphatidylcholine and of equimolar mixture of phosphatidylcholine and cholesterol.

Chapter II. Structural Parameters of Dipalmitoyl Phosphatidylcholine Lamellar Phase and Bilayer Phase Transitions

Thicknesses d_l of the lipid bilayer and d_w of the water layer were determined separately with X-rays for dipalmitoyl phosphatidylcholine lamellar phases. In both cases of the presence and the absence of excess water, d_l does not change appreciably at the pretransition (35°C) but drops down by about 5 Å at the main transition (42°C) with increasing temperature. In the presence of excess water, d_w jumps up by 4.0 Å at the pretransition and by 2.0 Å at the main transition. These results prove that there is practically no change of the tilting angle of hydrocarbon chains at the pretransition and that the remarkable increase of the repeat distance of the lamellar phase at the pretransition

in the presence of excess water is caused by the increase of the thickness of the water layer.

Chapter III. X-ray Diffraction Studies of Dipalmitoyl Phosphatidylcholine - Protein Complexes with Special Reference to Cytochrome b_5

X-ray diffraction studies have been made on lamellar phases of lipid-protein complexes. Proteins used in the studies were negatively charged proteins: the membrane protein cytochrome b_5 from rabbit liver microsomes and three non-membrane proteins (albumin, ovalbumin and β-lactoglobulin A). Lipid was dipalmitoyl phosphatidylcholine, which was charged positively by bound Ca^{2+}.

Repeat distances of the lamellar structures were determined. Modes of binding of the proteins to the lipid bilayers were examined through the profiles of the high-angle reflections and, in the case of cytochrome b_5, also through electron density projection onto the normal to bilayer. The bindings seem to be electrostatic in the cases of non-membrane proteins. For cytochrome b_5, the binding seems to be electrostatic when the complex is incubated below 35°C, and to be hydrophobic when incubated above 35°C. This critical temperature coincides with the pretransition temperature of dipalmitoyl phosphatidylcholine bilayer.

INTRODUCTION

First systematic studies of lipid-water systems were made by Luzzati et al. [1,2] on soaps and detergents in 1957 and later on biological lipids [3]. Then Reiss-Husson, Luzzati, Chapman and others made extensive studies on single lipids [4-6], mixed lipids [7-10] and total lipids extracted from biomembranes [3,11-13]. They found that lipid molecules aggregate in various modes in water, i.e., in micellar, cylindrical and bilayer forms. Among them the bilayer structure is the most common and appears in biomembranes.

The lipid bilayers assume several polymorphysm named as Lα, Lβ, Lβ' and Pβ' phases by Luzzati [6] and Tardieu [14]. These phases are related with arrangements of hydrocarbon chains, as illustrated in Fig.A-2 of Appendix.

In water most lipid bilayers have a tendency to form the so-called lamellar phase in which the bilayers and water layers are stacked alternately, giving a well-defined repeat distance. There had been, however, no very definite evidence of what factors determine the repeat distance. Basic data for this problem are presented in Chapter I. Recently these data have been used for analysis of interbilayer interactions with considerable success [15].

LeNeveau et al. [16,17] demonstrated that lipid bilayers have rather rigid hydration layers on their surfaces. Chapter II describes how the hydration layers change asso-

ciated with the phase transitions in dipalmitoyl phosphatidylcholine bilayer.

Lipid-protein complexes were investigated by several authors [18-23]. The proteins used so far are, however, limited to non-membrane proteins. Chapter III gives data on lamellar phase of the membrane protein, cytochrome b_5 and dipalmitoyl phosphatidylcholine bilayer in comparison with other lipid-protein complexes.

CHAPTER I

EFFECTS OF CATIONS ON DIPALMITOYL PHOSPHATIDYLCHOLINE - CHOLESTEROL - WATER SYSTEMS

I-1 Introduction

The inter-membrane interactions which produce the lamellar phase in lipid-water systems seem to have close connection with inter-cell interactions and have been discussed by several workers. The van der Waals forces will be an origin of attractive forces and there must be an electrostatic repulsive force if the head groups have net electric charges, as discussed by parsegian [24-26]. One experimental approach to this problem might be to investigate the effects of net charges on the membrane, and another to change the physical and chemical properties of water by introducing solutes such as electrolytes. Gulik-Krzywicki et al. [27] demonstrated that the repeat distance of the lamellar phase increases remarkably when lipids bearing net charge are added to egg-yolk lecithin. Palmer et al. [28] observed that the lamellar phase of lipid extracted from beef spinal cord disappears at the $CaCl_2$ concentration of 60 mM. Also several workers [27-30] reported that parameters which define lamellar structures are varied when electrolytes are added to water. More detailed studies, however, seem to be

needed to clarify the roles of electrolytes in water. This chapter reports our results on the effects of electrolytes upon dipalmitoyl phosphatidylcholine-cholesterol-water systems, with special emphasis on $CaCl_2$.

I-2 Materials and Methods

Material preparation

Synthetic β,γ-dipalmitoyl-D,L-(α)-phosphatidylcholine (DPPC) was purchased from Sigma Chemical Co., and cholesterol from Nakarai Chemicals Ltd. These chemicals were used without further purification. Phosphatidylcholine and cholesterol were dissolved in chloroform at a concentration of 2 mM and were stored at -20°C.

These solutions were mixed at the desired molar ratio of DPPC and cholesterol. These mixtures were dried with rotary evaporator at about 40°C, and then the remaining chloroform was futher evaporated by keeping the specimen in an evacuated desiccator for at least 1 h. The dried lipids were dispersed in aqueous solutions of LiCl, NaCl, KCl, $MgCl_2$, $CaCl_2$, $SrCl_2$ and $BaCl_2$. Ample solution was used, so that there always existed excess water phase together with the lamellar phase.

The dispersions were sealed in thin-walled glass capillaries having 1.0 mm internal diameter. The density of solution becomes comparable to, and then larger than, that

of membrane with increasing concentration of the salt. Therefore, to produce a region which is rich in lamellar phase in the capillary, the dispersions were centrifuged at 30 000 × g for 30 min by holding the capillary in the hole of a modified centrifuge tube filled with 0.5 M sucrose solution.

X-ray diffraction techniques

The glass capillary was placed on the brass sample holder maintained at about 5°C. X-ray diffraction patterns were recorded on Fuji Medical KX X-ray films ($5 \times 5\ cm^2$) using Ni-filtered Cu Kα radiation ($\lambda = 1.542\ \text{Å}$) from a Rigaku Denki rotating anode microfocus generator. Exposures were made on an Elliott toroidal and a Franks point focusing cameras, operated in vacuum. Sample-to-film distances were varied from 48 to 78 mm according to the desired scattering angle region. Exposure time was between 4 and 60 h. Diffraction spacings were calibrated with $Pb(NO_3)_2$ and sodium myristate powder patterns. Microdensitometer tracings of the films were done on a Nalumi type C microdensitometer. Ambiguity of measured spacing was within ± 0.5 Å.

I-3 Results

Four states in $CaCl_2$ solutions

X-ray photographs of DPPC-water systems were taken at

various concentrations of $CaCl_2$ between 0 and 1 M. Results obtained revealed that there are basically four different states depending upon the $CaCl_2$ concentration, which will be called I, II, III and IV below. Fig.I-1 shows typical diffraction patterns for them. Characteristic of the four states are as follows.

State I appears in the $CaCl_2$ concentration range of $0 \sim 1$ mM. It consists of the lamellar phase and excess water phase. Fig.I-1a shows a diffraction pattern from the lamellar phase. The repeat distance of the phase is practically independent of $CaCl_2$ concentration and is about 64.5 Å.

State II appears in the concentration range of $1 \sim 10$ mM. Here the lipid-rich phase swells into the excess water. Fig.I-1b shows the diffraction pattern, which gives only diffuse peaks in low-angle region, whereas sharp high-angle (~ 4 Å) lines persist. The low-angle diffraction patterns

---

Fig.I-1. X-ray diffraction photographs of DPPC-water systems taken at 5°C. Large rings correspond to a spacing of about 4 Å. A Franks point focusing camera was used for taking (a), (c) and (d), and an Elliott toroidal point focusing camera for (b). (a) Lamellar phase of State I in pure water; repeat distance d = 64.5 Å: (b) State II, at 5 mM $CaCl_2$. (c) Lamellar phase in State III at 50 mM $CaCl_2$; d = 120 Å. (d) Lamellar phase in State IV at 0.5 M $CaCl_2$; d = 64.5 Å. (For definition of these states, see the text.)

Fig. I-1

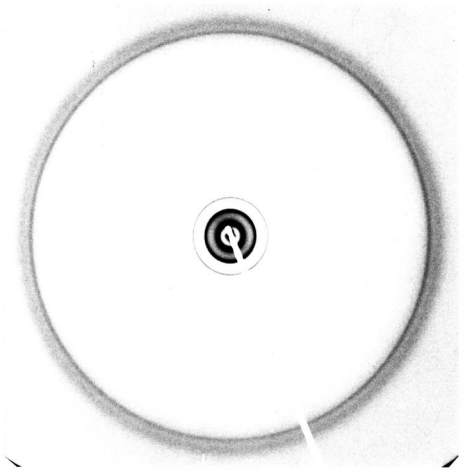

a

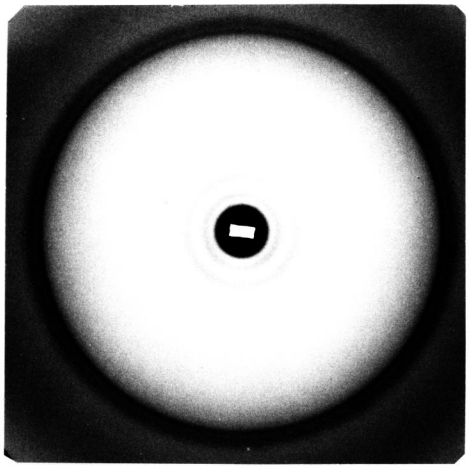

b

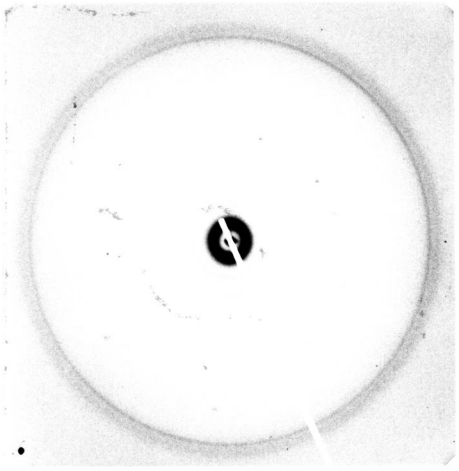

c

d

are similar to that obtained from sonicated dispersions of egg-yolk lecithin in water reported by Wilkins et al. [31], suggesting that State II corresponds to dispersion of lipid bilayers. Autocorrelation function and profile of electron density calculated with the diffuse peaks supported this model.

State III appears in the concentration range of 10 ∿ 200 mM. Here again the excess water phase coexists. Fig.I-1c shows the diffraction pattern which gives two low-angle diffraction lines, though they are not very sharp. The two low-angle lines can be indexed assuming lamellar structure with a large repeat distance. This indicates the reappearance of a partially disordered lamellar phase.

State IV appears at concentrations greater than 200 mM. Fig.I-1d shows the diffraction pattern, which is quite similar to that in Fig.I-1a, but the lines are sharper and background lower than those in Fig.I-1a, suggesting that the lamellar structure has more perfect order.

Diffraction patterns from the same lipids in solutions of different $CaCl_2$ concentrations revealed that the transitions between the four states are reversible. In these experiments the lipids were washed by repeated replacements of solutions of new concentration. To reobtain samples free of Ca^{2+}, 10 mM EDTA was used.

Similarly, dispersions of mixtures of DPPC and cholesterol were examined up to the molar ratio of chole-

Fig.I-2

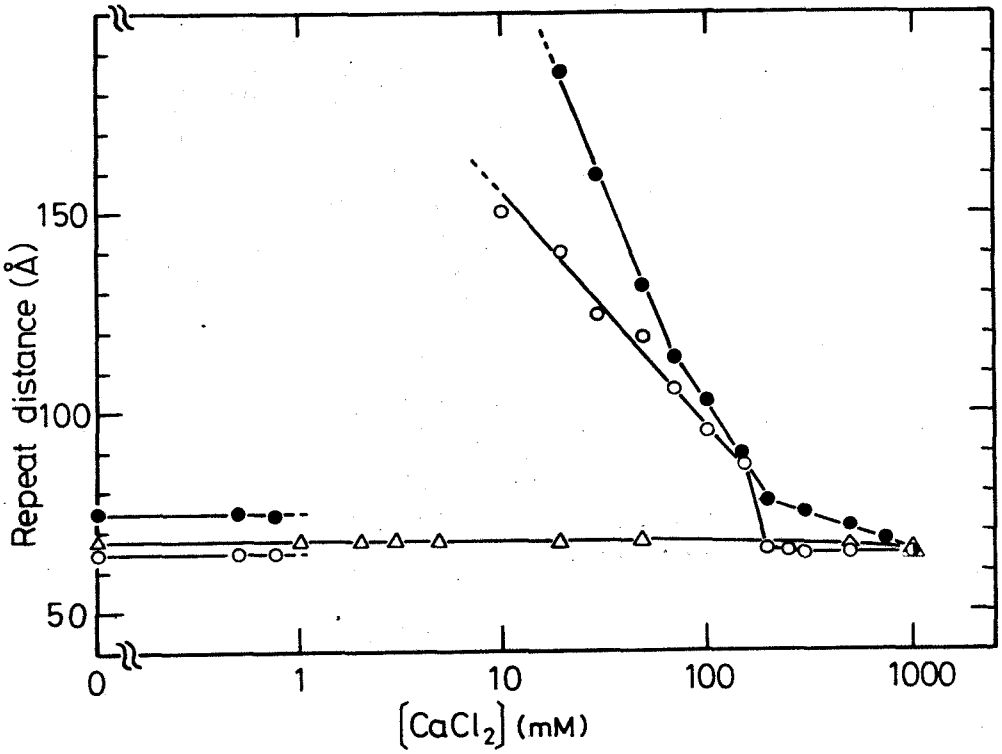

Fig.I-2. Repeat distances d of the lamellar phase as functions of $CaCl_2$ concentration for various molar ratios of cholesterol/ phosphatidylcholine. ○ , 0/10; ● ,2/8; △ , 5/5.

sterol of 50%, beyond which crystalline cholesterol precipitated. The effects of Ca^{2+} were similar those in the case of pure DPPC on the whole. The $CaCl_2$ concentration at which the I – II transition takes place tends to increases with molar ratio of cholesterol/DPPC: 1 mM for ratio 0/10, 1 mM for 2/8, 5 mM for 3/7, 50 mM for 4/6. When the ratio reaches 5/5, no transition was observed.

Fig.I-2 shows repeat distances of the lamellar phases as functions of $CaCl_2$ concentration. The curves correspond to the molar ratio of cholesterol/DPPC of 0/10, 2/8 and 5/5.

$CaCl_2$ exhibits the similar effects on dimyristoyl phosphatidylcholine (DMPC) but no effects on egg-yolk lecithin.

Changes in high-angle reflections with $CaCl_2$ concentration

The high-angle reflections corresponding to spacing of about 4 Å changes their profiles with $CaCl_2$ concentration and cholesterol content as shown in Fig.I-3. In the absence of cholesterol, the profiles are characterized by a 4.2 Å sharp reflection followed a diffuse peak [14] as shown in Curve a up to 0.5 M $CaCl_2$. At a high concentration above 0.5 M, three peaks appear as shown in Curve a', indicating the molecular rearrangement in bilayers.

Addition of cholesterol makes the diffraction lines diffuse in pure water as seen in Curves b, c, d and e, as also reported by other authors [9], but three peaks appear as seen in Curves b', c' and d' at high $CaCl_2$ concentration.

Fig. I-3

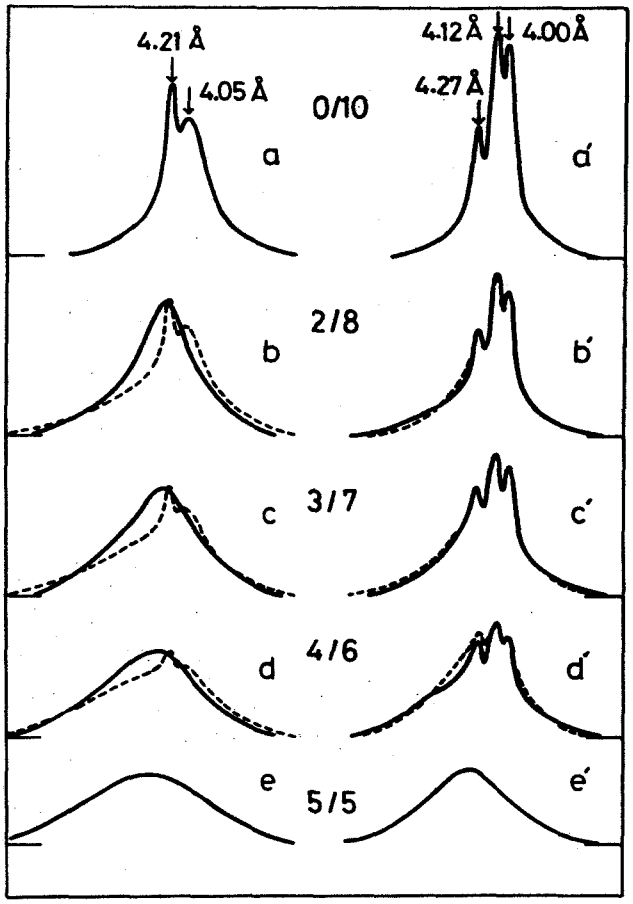

Fig. I-3. Profiles of high-angle reflections at 5°C. a, b, c, d and e, in pure water; a', in 0.5 M $CaCl_2$ solution; b', c', d' and e', in 1 M $CaCl_2$ solutions. The fractions in the figure indicate the molar ratios of cholesterol/Phosphstidylcholine. Spacing of the peaks are also given. The dotted lines show superpositions of a and e on the left-hand side, and of a' and e' on the right-hand side at the ratio of $(c_p - c_c)/2c_c$.

Positions of these three peaks do not depend upon $CaCl_2$ concentration and cholesterol content. The general feature of Curves b', c' and d' can be reproduced by a superposition of a' and e' at the ratio of $(c_p - c_c)/2c_c$, where c_p and c_c are molar concentrations of DPPC and cholesterol. For the equimolar mixture of DPPC and cholesterol, a single diffuse peak was observed at all $CaCl_2$ concentrations examined, as shown in Curves e and e'.

Effects of cations other than Ca^{2+}

Effects of additions of LiCl, NaCl, KCl, $MgCl_2$, $SrCl_2$ and $BaCl_2$ on DPPC-water system were studied in the same manner as for $CaCl_2$. Pronounced changes in diffraction patterns were also observed for $MgCl_2$. In this case, however, State I is directly followed by State III, which is succeeded by State IV. High-angle reflections did not change appreciably, that is, the peaks such as shown on the right-hand side of Fig.I-3 were not observed at all $MgCl_2$ concentrations up to 1 M. The observed repeat distance of the lamellar phase is given as a function of $MgCl_2$ concentration in Fig.I-4. The other salts exhibited practically no effect by themselves.

All the above mentioned salts produced States III and IV from State II induced by 5 mM $CaCl_2$. Their effects are similar to that of Ca^{2+} in this respect. The concentrations where the transition III→IV occurs are 50 mM for $BaCl_2$,

Fig. I-4

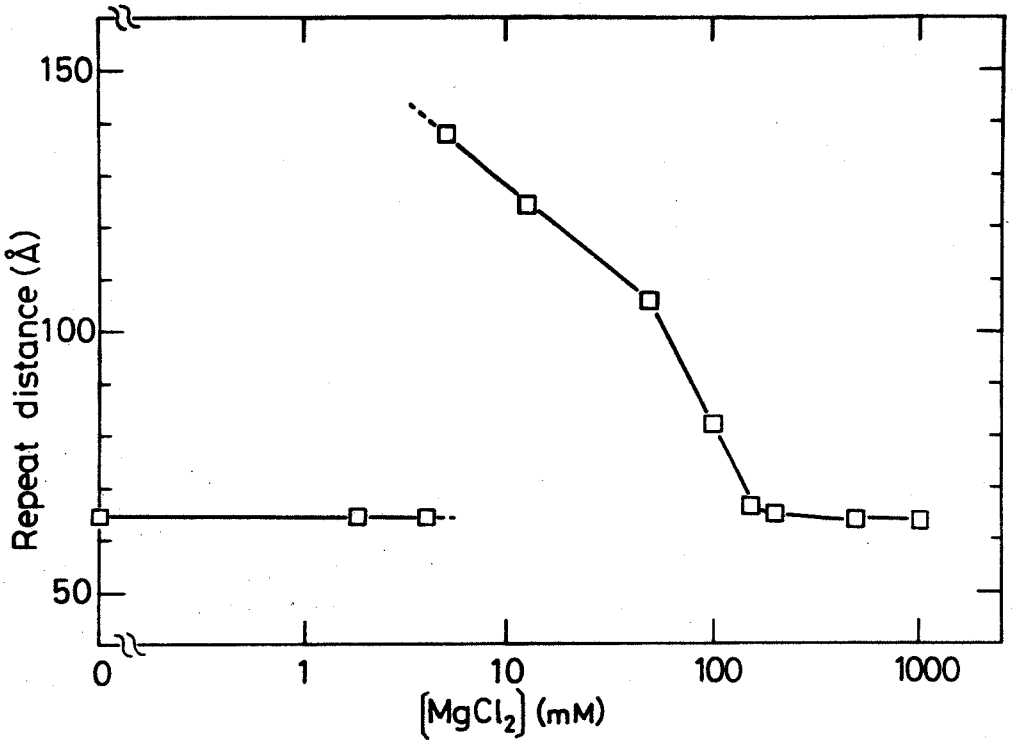

Fig.I-4. Repeat distance d of the lamellar phase of pure phosphatidylcholine as a function of $MgCl_2$ concentration.

100 mM for KCl and $SrCl_2$, 125 mM for NaCl and 200 mM for LiCl, $MgCl_2$ and $CaCl_2$.

I-4 Discussion

The results obtained may be summarized as follows.

(1) $CaCl_2$ induces the States II, III and IV and $MgCl_2$ States III and IV.

(2) The salts LiCl, NaCl, KCl, $MgCl_2$, $CaCl_2$, $SrCl_2$ and $BaCl_2$ produce the States III and IV when they are added to the State II induced by 5 mM $CaCl_2$.

(3) At high $CaCl_2$ concentrations, three peaks were observed in high angles when the molar ratio of cholesterol/DPPC is less than 5/5, as shown in Fig.I-3.

(4) The Curves b', c' and d' in Fig.I-3 can be reproduced by superposition of a' and e' at the ratio of $(c_p - c_c)/2c_c$.

(5) Cholesterol in the bilayers tends to stabilize the lamellar phase against the effects of electrolytes.

Recently, Furuya et al. [32] have observed that uranyl acetate induces only the State II in which the lipid-rich phase swells into the water phase. The effect of this salt is very strong: the critical molar ratio of uranyl acetate/DPPC to produce the transition is between 1/800 and 1/400 [32], that is, the transition occurs when about 2 per 10^3 DPPC molecules bind the uranyl ions. Also, the affinity of

uranyl ions to DPPC is very large: titration measurement [32] proved that the water phase is almost free of uranyl ions when the molar ratio of uranyl acetate/DPPC is less than 1 in the whole system. Structural analysis [32] of DPPC bilayers decorated with equimoar uranyl ions has revealed that the uranyl ions sit near the head groups of DPPC molecules.

All these observations suggest that ions bound at membrane surfaces cause repulsive forces between membranes and tend to induce State II . Studies on phosphatidylcholine monolayers indicated that dipalmitoyl phosphatidylcholine is able to bind more Ca^{2+} than egg-yolk lecithin or oleoyl phosphatidylcholine [33,34] but its ability is less than that of phosphatidylethanolamine and far less than that of phosphatidylserine [35]. These imply that some ions are bound by bilayers and others are free in water in the case of $CaCl_2$ and the situation may be more or less similar for the above-mentioned inorganic salts. Results (1) suggest that competing attractive and repulsive forces operate over tens of Angstrom between membranes. Therefore, the inter-membrane distance is given by a distance where the two forces balance. Here, the attractive force will be caused by a van der Waals interactions between membranes. $CaCl_2$ and $MgCl_2$ induce State II and III from I, respectively. These transitions are associated with increase of inter-membrane distance. Therefore, the bound ions may be respon-

sible for these transitions. In the case of $CaCl_2$, State III appears with further increase of concentration. Figs I-2 and 4 indicate that in State III the inter-membrane distance decreases and therefore the attractive forces between membranes increase relatively to the repulsive forces with increasing $CaCl_2$ and $MgCl_2$ concentrations. It seems possible that these phenomena are related to the existence of free ions in water. Recently, Ohshima and Mitsui [15] have explained quantitatively these phenomena on the basis of the DLVO theory of colloidal stability. Also they have explained why the transition from I to II is so abrupt and why the disordered dispersion (State II) is more stable than the lamellar structures. Results (2) suggest that all inorganic salts examined tend to increase attractive force between membranes relatively to the repulsion from some concentrations. Fig.I-5 is a schematic representation of the sequence of structural transformations among the four states I, II, III and IV.

The Lβ' phase [14] in which the hydrocarbon chains are tilted to the membrane plane gives the high-angle peak profile similar to Curve a in Fig.I-3 (cf. Fig.11d of ref.14). In the Lβ phase the hydrocarbon chains are perpendicular to the membrane [11,14]. If the chain can be regarded as a cylinder, close packing of them results in a two-dimentional hexagonal lattice in the membrane [14]. Now let us consider a general two-dimensional unit cell of which the edges are

Fig. I-5

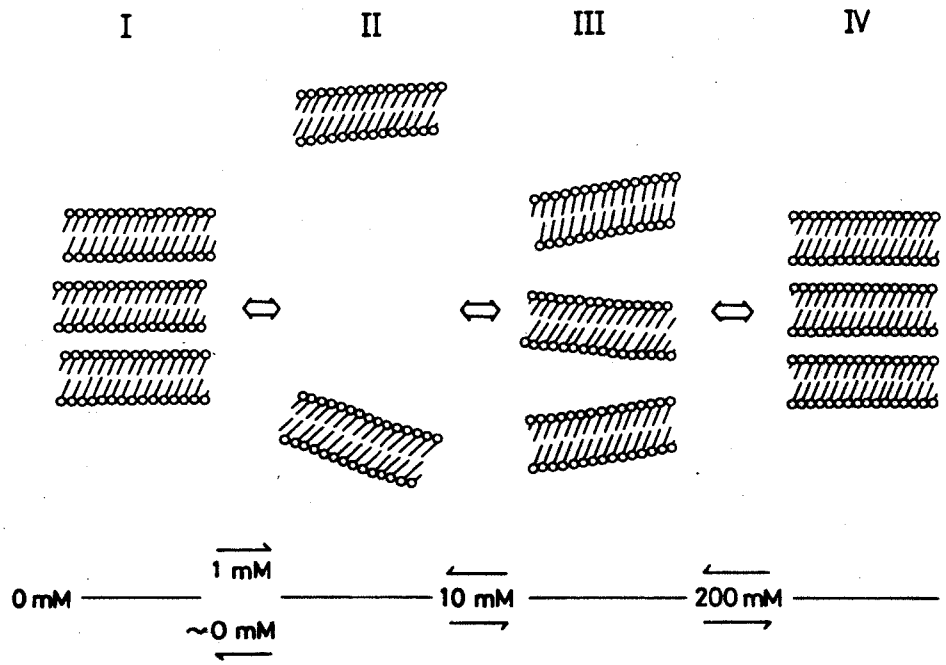

Fig.I-5. Schematic representation of the four states I, II, III and IV. Values in units of mM give the $CaCl_2$ concentration at which the transition between two states occurs.

a and b and the angle is γ. The hexagonal lattice is characterized by a single parameter a, since $b = a$, $\gamma = 120^\circ$, and thus there will appear a single sharp peak around the 4 Å region (cf. Fig.11b of ref.14). In actual phosphatidylcholine molecules, two hydrocarbon chains are paired by the head group. This implies that the hexagonal unit cell with $a \simeq 4 \cdot (2/\sqrt{3})$ Å contains half a molecular unit of the head group. Such a situation can happen only when the arrangement of the head groups is disordered, keeping the hexagonal symmetry in an averaged structure. It is well known that crystals that have high symmetry due to partial disorder tend to transform into other crystal forms of lower symmetry with changes of external parameters such as temperature and pressure. By analogy, it seems possible that a phase having symmetry lower than hexagonal can appear in the membrane at some $CaCl_2$ concentration. It is easy to prove that a non-hexagonal lattice can bring about a group of three diffraction peaks around the 4 Å region corresponding to the three lattice parameters if deviations from the hexagonal lattice are appropriate, as actually observed and shown on the right-hand side of Fig.I-3. Therefore, the Results (3) imply that the structures of bilayers at high $CaCl_2$ concentrations are different from the usual model of $L\beta$.

Results (4) seem to be related to the phase separation. Generally, in studies of the phase diagram of materials A and B, the uniform mixed-crystal phase is recognized by

a shift of diffraction peaks of A with increasing B concentration. On the other hand, coexistence of A and B phases (or of A phase and an equimolar mixture A-B phase, etc.) is characterized by a superposition of diffraction peaks originated from the two phases. The contribution of each phase to the diffraction pattern is proportional to the amount of material in it. If a pure DPPC phase and an equimolar DPPC/cholesterol phase coexist in membranes, the ratio of materials in the two phases is approximately $(c_p - c_c)/2c_c$. Therefore, Results (4) suggest coexistence of the pure DPPC phase which gives the diffraction pattern a' in Fig.I-3 and of the equimolar DPPC/cholesterol phase of which the diffraction pattern is e'. No agreement between the solid and dotted lines was obtained on the left-hand side of Fig.I-3, suggesting that a well defined phase separation does not occur in pure water at 5°C. These results, however, do not deny the possibility of the local phase separation, which can not be detected with X-rays, and in this sense they do not necessarily contradict the reports on phase separations by several authors [36-39].

Concerning the results (5), the transition from I to II occurs at almost the same $CaCl_2$ concentration ($\sim$1 mM) for cholesterol/DPPC mixtures of 0/10 and 2/8, as seen in Fig.I-2. Beyond this molar ratio, the transition occurs at 5 mM for the ratio 3/7, 50 mM for 4/6, and no transition was observed for 5/5. These results suggest that affinity of

Ca^{2+} to the membranes tends to decreases with increasing cholesterol content and also that cholesterol prevents the binding of Ca^{2+} to phosphatidylcholine, as was discussed by Shah and Schulman [40] in case of egg-yolk lecithin monolayers.

I-5 Summary

(1) Addition of 1 mM $CaCl_2$ to DPPC-water system destroys the lamellar structure with a repeat distance of 64.5 Å and makes it swell into excess water.

(2) The lamellar phase reappears when $CaCl_2$ concentration increases: a partially disordered lamellar phase with the repeat distance of 150 ∿ 200 Å comes out the concentration of about 10 mM, the lamellar diffraction patterns become sharp and repeat distance decreases with increasing $CaCl_2$ concentration. The repeat distance above 200 mM is the same as that in pure water.

(3) $MgCl_2$ induces the lamellar phase of large repeat distance, whereas LiCl, NaCl, KCl, $SrCl_2$ and $BaCl_2$ exhibit practically no effects on the lamellar structure by themselves.

(4) Addition of more than 0.5 M $CaCl_2$ causes rearrangements of the molecules in DPPC bilayer.

(5) Incorporation of cholesterol into DPPC bilayers tends to stabilize the lamellar phase. At high $CaCl_2$ concentrations, this mixed bilayers consist of two phases of pure DPPC and of equimolar DPPC and cholesterol.

CHAPTER II

STRUCTURAL PARAMETERS OF DIPALMITOYL PHOSPHATIDYLCHOLINE LAMELLAR PHASES AND BILAYER PHASE TRANSITIONS

II-1 Introduction

Bilayers of dipalmitoyl phosphatidylcholine (DPPC) exhibit phase transitions at 35°C and 42°C in water [5,41]. The transition at 35°C is evidenced by a small anomaly of the specific heat and called a pretransition. Rand et al. [42] proposed that the intermediate phase between 35°C and 42°C is of the type of Lβ, whereas Janiak et al. [43] proposed that it is Pβ'. Additional data are supplied on this phase and comments are given on their models in this chapter. The transition at 42°C is associated with a pronounced anomaly of the specific heat and called a main transition, which is of the order-disorder type as evidenced by distinct changes in X-ray diffraction pattern [5, 42-44]. Transitions of these two types take place also in bilayers of dimyristoyl phosphatidylcholine (DMPC) and other synthetic lecithins having two saturated hydrocarbon chains [5,41].

Bilayers of DPPC form the lamellar phase in water. Recently Rand et al. [42] have reported that in water the repeat distance of the lamellar phase changes remarkably at the two transition points. We had observed the same phenomena independently and have tried to determine which is respon-

sible to the changes, the lipid layer or the water layer. This chapter reports our results concerning this problem. Also recent experimental and theoretical studies [45 ,15-17] of the lamellar phase established that the water layer in the lamellar phase can be regarded as a pair of hydration layers on lipid bilayers in pure water or in aqueous solution of 1 M $CaCl_2$. This chapter thus provides information on variation of the hydration layers on lipid bilayer associated with its phase transitions.

II-2 Materials and Methods

Synthetic β,γ-dipalmitoyl-D,L-(α)- and β,γ-dimyristoyl -L-(α)-phosphatidylcholine (DPPC and DMPC) were obtained from Sigma Chemical Co. Four kinds of specimens were prepared: wet pellets, and lipid bilayers in water, in aqueous solution of 5 mM $CaCl_2$ and 1 M $CaCl_2$. The wet pellets were made by controlling weight ratio c' of lipid/(lipid + water) in the range of $0.5 \sim 0.8$. The lipid was dissolved in chloroform and the solution was dried in a stream of N_2 gas. The remaining lipid was kept in an evacuated desiccator for at least 1 h for complete dryness. It was then sealed with water at various ratios c' in ampoules. These specimens were kept at about 50°C for about three days to make them form a uniform mixture. The other specimens mentioned above were prepared by putting the dried lipid in water or in aqueous solutions of $CaCl_2$. Deionized and distilled water was used.

For X-ray studies the specimens were taken out from ampoules and sealed in thin-walled glass capillaries having the internal diameter of 1.0 ∿ 2.0 mm. The capillary was set on a brass sample holder. Its temperature was changed in the range of 5 ∿ 55°C by flowing water through the holder. Temperature of the water was controlled within the accuracy of ± 0.2°C with thermoelectric elements. A thermocouple pasted on the sample holder served to measure the temperature.

X-ray diffraction patterns were recorded on Fuji Medical KX X-ray films ($5 \times 5\ cm^2$) using Ni-filtered Cu Kα radiation ($\lambda = 1.542\ \mathring{A}$) from a Rigaku Denki rotating anode microfocus generator. An Elliott toroidal focusing optics was used in vacuum. Sample-to-film distances were changed in the range of 48 ∿ 78 mm. The spacings were calibrated with $Pb(NO_3)_2$ powder. Exposure time was about 2 h for the lamellar structures and about 20 h for the dispersions. Optical densities of the films were measured by a microdensitometer. Non-linearity between the density and X-ray intensity was corrected by a standard scale.

II-3 Experimental Results

X-ray observations indicated that the wet pellets consisted of lamellar phases having uniform repeat distance. The lipid bilayers in water or in the solution of 1 M $CaCl_2$ consisted of lamellar phases and excess water or solution. The lipid

bilayers were uniformly dispersed in the aqueous solution of 5 mM $CaCl_2$ without forming the lamellar phase, as was observed before [45] (see the preceding chapter).

Fig.II-1a and b respectively show the repeat distances d_1 of DPPC and DMPC lamellar structures as functions of temperature T. The open circles represent the data obtained in the presence of excess water. With rising temperature, the repeat distance jumps up by about 5.0 Å at the pretransition and drops down by about 2.5 Å at the main transition for both DPPC and DMPC, in fairly good agreement with the results reported by Rand et al. [42] for DPPC. (The value of 77 Å in their Table 1 seems to be a misprint of 70 Å given on p.1119 of their paper.) The filled circles and squares in Fig.II-1 stand for the repeat distances of the wet specimens in the absence of excess water. In these cases no distinct discontinuous changes were observed around 35°C, whereas the discontinuous drop was more distinct at the main transition than in the presence of excess water.

Fig.II-2 shows repeat distances d in the wet pellets as functions of water content 1-c' for 5°C, 37°C and 45°C. In Fig.II-2c two data points in parentheses were neglected in drawing the curve because there seemed to be a possibility of existence of small water drops isolated from the lipid-water lamellar phases in the capillaries. Each curve in Fig.II-2 demonstrates that there is a critical value of 1-c' above which d remains constant as reported by several

Fig. II-1

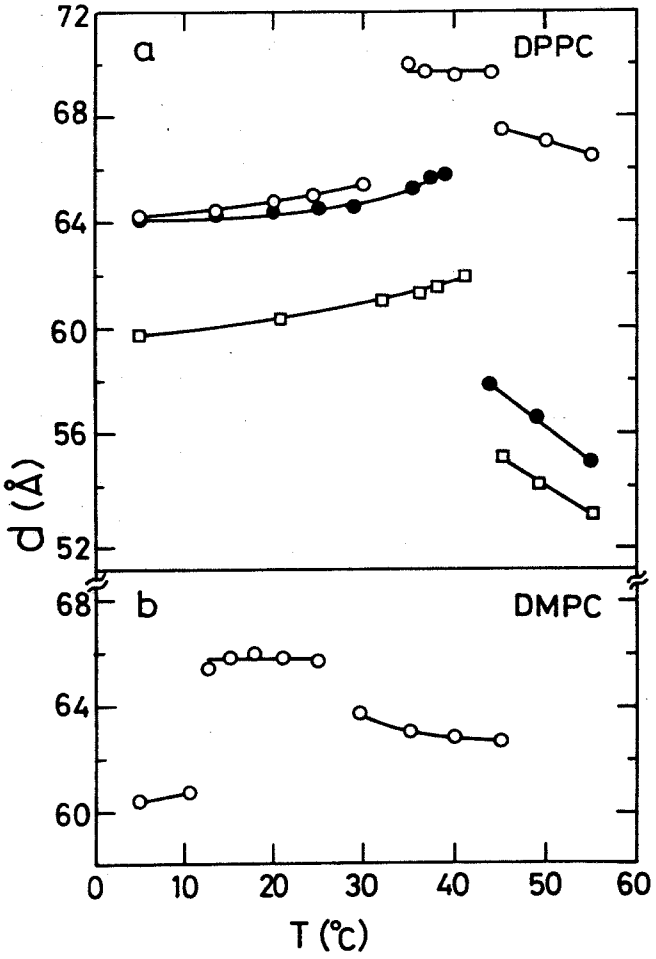

Fig.II-1. Repeat distances d of the lamellar phases as functions of temperature T. (a) DPPC. ○, in the presence of excess water; ●, c' = 0.7; □, c' = 0.8. (b) DMPC in the presence of excess water.

Fig. II-2

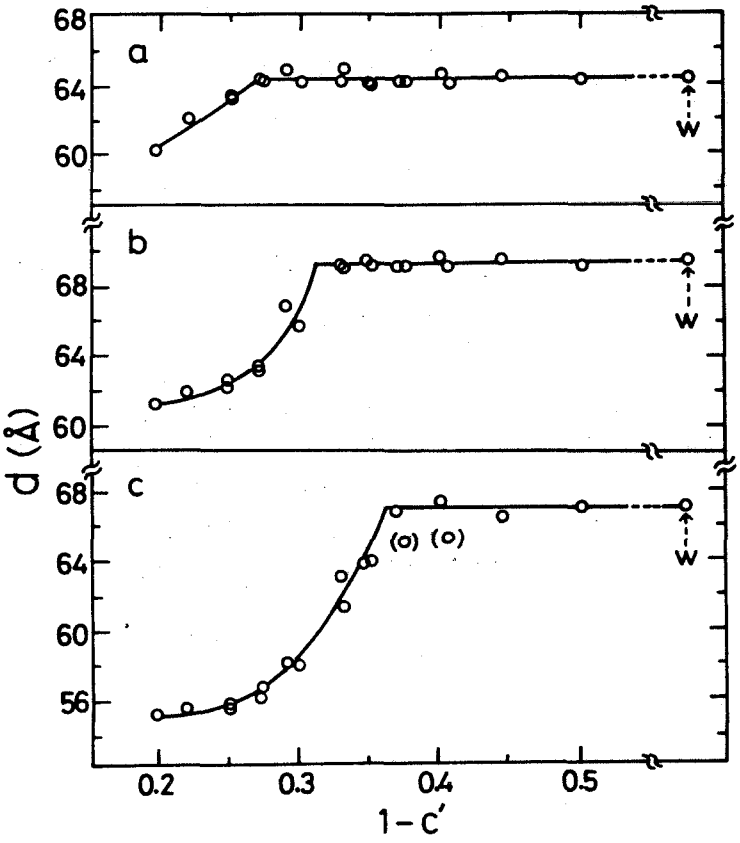

Fig.II-2. Repeat distances d of DPPC lamellar phases as functions of water content 1 - c'. (a) 5°C; (b) 37°C; (c) 45°C.

Fig. II-3

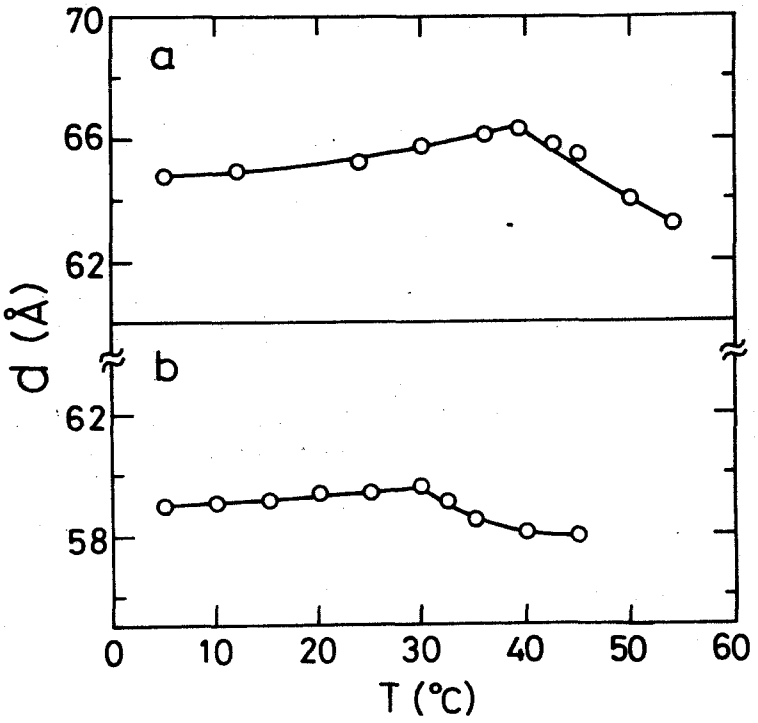

Fig.II-3. Repeat distances d of the lamellar phases in aqueous solution of 1 M $CaCl_2$ as functions of temperature T. (a) DPPC; (b) DMPC.

authors [5,46-48]. The critical value of c' and the constant value of d will be denoted as c* and d*, respectively. Fig.II-2 indicates that c* = 0.73, d* = 64.5 Å at 5°C, c* = 0.69, d* = 69.5 Å at 37°C and c* = 0.64, d* = 67.5 Å at 45°C. Excess water is expected to have existed for c' < c* although it could not be recognized by eyes. The data points marked by w were obtained for the lamellar phases in distinct presence of excess water.

In the intermediate phase between the pre- and main transitions, there appeared additional reflections c' > c* as reported by Janiak et al.[43].

Fig.II-3 shows the repeat distances d of DPPC and DMPC lamellar structures in aqueous solution of 1 M $CaCl_2$ as functions of temperature. In spite of the presence of excess solution, there are no discontinuous changes in d itself unlike the case in pure water, although there appear discontinuous changes in tangents of the curves of d vs. T at 39°C for DPPC and at 30°C for DMPC. Above these temperatures the high-angle reflection becomes diffuse with a peak at 4.6 Å proving that the bilayer structure is disordered. Therefore, these temperatures should be regarded as the main transition temperature.

As stated above, DPPC bilayers in aqueous solution of 5 mM $CaCl_2$ did not form lamellar structures, and gave continuous diffraction patterns. Fig.II-4 shows these patterns.at 5°C, 37°C and 45°C. Fig.II-5 shows the

Fig. II-4

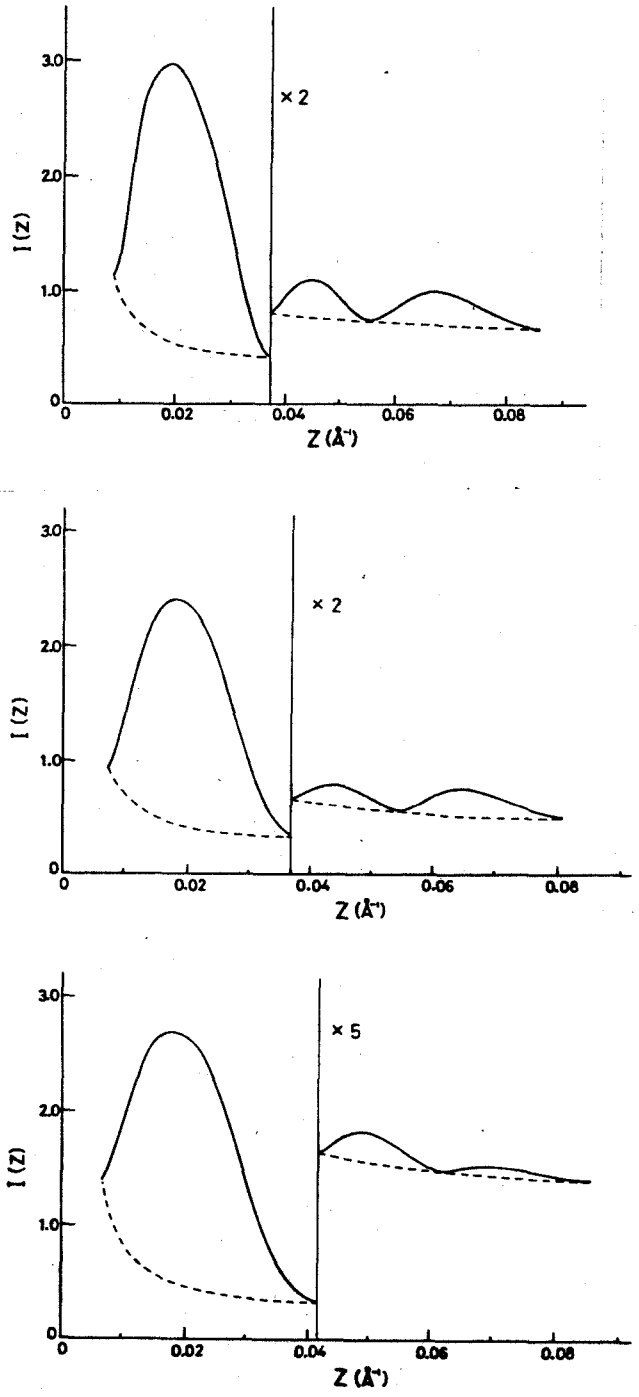

Fig.II-4. Scattering curves for dispersions of single DPPC bilayers at three temperatures. Dotted curves are background and incoherent scattering. (a) 5°C; (b) 37°C; (c) 45°C.

Fig. II-5

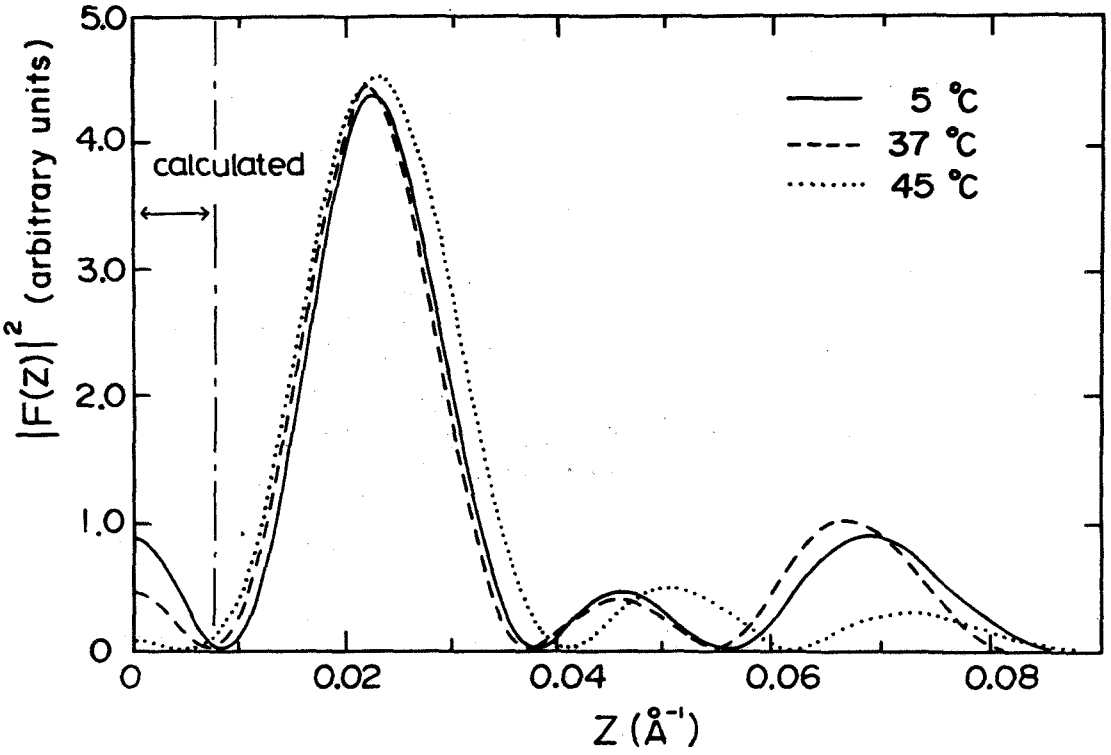

Fig.II-5. Corrected intensity $|F(Z)|^2$ of a single DPPC bilayer at three temperatures. Each curve was normalized with $\int |F(Z)|^2 dZ=100$. ——, 5°C; - - - - , 37°C; ....., 45°C.

intensities $|F(Z)|^2$, corrected for background and incoherent scattering, where F(Z) is the scattering amplitude of a single bilayer and Z is the reciprocal coordinate perpendicular to the bilayer and related to the scattering angle 2θ by $Z = 2\sin\theta/\lambda$. Values of $|F(Z)|^2$ were calculated from the observed intensity I(Z) by the equation of $|F(Z)|^2 = Z^2 I(Z)$. It was difficult to obtain I(Z) for $Z < 0.009\ \mathring{A}^{-1}$. The values given in this region in Fig.II-5 are calculated as described in next section.

II-4 Calculations

Here we define the weight ratio c and the volume ratio c_v of lipid as lipid/(lipid + water) in the lamellar phase, excluding the contribution from the excess water. Fig.II-2 suggests that the water content in the lamellar phase is satulated for $c' \leq c^*$, and thus $c = c'$ for $c' > c^*$ and $c = c^*$ for $c' < c^*$. Therefore, by using the values of c^* given in Section II-3, we have c of DPPC lamellar phases in the presence of excess water, as listed in Table II-1. The volume ratio c_v is given by $c_v = c\bar{v}_l/\{c\bar{v}_l + (1-c)\bar{v}_w\}$, where $\bar{v}_l$ and $\bar{v}_w$ are specific volumes of the lipid and water, respectively. Now we define thickness of the lipid bilayer d_l and thickness of the water layer d_w in the lamellar phase by $d_l = c_v d$ and $d_w = (1-c_v)d$, respectively. Values of $\bar{v}_l$ were calculated from molar volumes given for $27 \sim 45°C$

Table II-1

Parameters in DPPC Lamellar Phase at Three Temperatures, in the Presence of Excess Water

T (°C)	c (wt/wt)	$\bar{v}_l$ a) ($cm^3 g^{-1}$)	$\bar{v}_w$ b) ($cm^3 g^{-1}$)	d (Å)	d_l (Å)	d_w (Å)
5	0.73	0.944	1.000	64.2	46.1	18.1
37	0.69	0.957	1.007	69.7	47.3	22.4
45	0.64	1.004	1.010	67.5	43.1	24.4

a) Calculated from the data given in the reference 49. b) Taken from the reference 50.

Fig.II-6

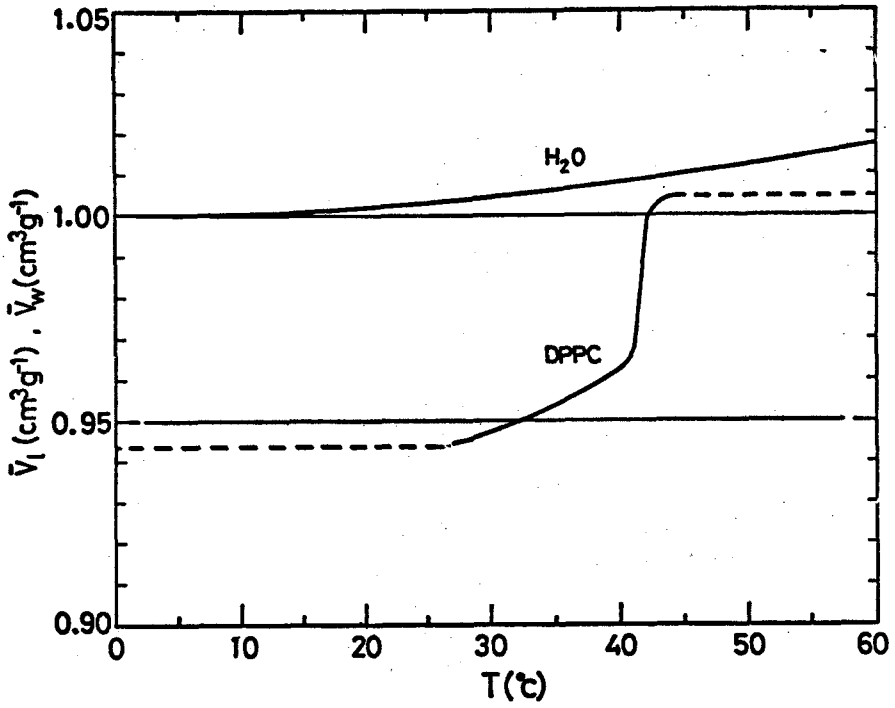

Fig.II-6. Parameters $\bar{v}_l$ and $\bar{v}_w$ as functions of temperature T. Values of $\bar{v}_l$ were calculated from the data given for 27 ∿ 45°C by Sheetz and Chan [49], with a extension (the dotted lines) outside the temperature region. Values of $\bar{v}_w$ were taken from Handbook [50].

by Sheetz and Chan [49], with a extension outside the temperature region. Values of $\bar{v}_w$ were taken from Handbook[50]. They are plotted in Fig.II-6. Table II-1 gives the calculated values of d_l and d_w at 5°C, 37°C and 45°C together with other parameters. We calculated d_l and d_w at other temperatures on the assumption that c is constant and equal to the values at 5°C, 37°C and 45°C in the three phases, respectively. Fig.II-7 shows results together with d given in Fig.II-1a.

Naturally decrease of d_l causes increase in area of bilayers. Thus it will cause decrease of d_w in the wet specimens of $c' > c^*$ since there is no water supply into the lamellar phase. Calculations of d_l and d_w were made for these causes by using the relationships; $d_l = c_v d$, $d_w = (1-c_v) \times d$, $c_v = c\bar{v}_l / \{ c\bar{v}_l + (1-c)\bar{v}_w \}$. Fig.II-8 shows results for $c' = 0.8$ together with d given in Fig.II-1a.

As demonstrated by Furuya et al. [32], continuous diffraction intensities as shown in Fig.II-5 can give the electron density projection $\rho(z)$ onto the normal to lipid bilayer with less ambiguity in the phases of F(Z) than the lamellar reflections. Experimental intensity data were, however, lacking in the small-angle region of $Z < 0.009\ \mathring{A}^{-1}$ as mentioned in Section II-3. To supply F(Z) in this region we examined various step function models with six parameters [32]. The best-fit model (Table II-2) gave the discrepancy factor R of 0.035 for the experimentally

Fig. II-7

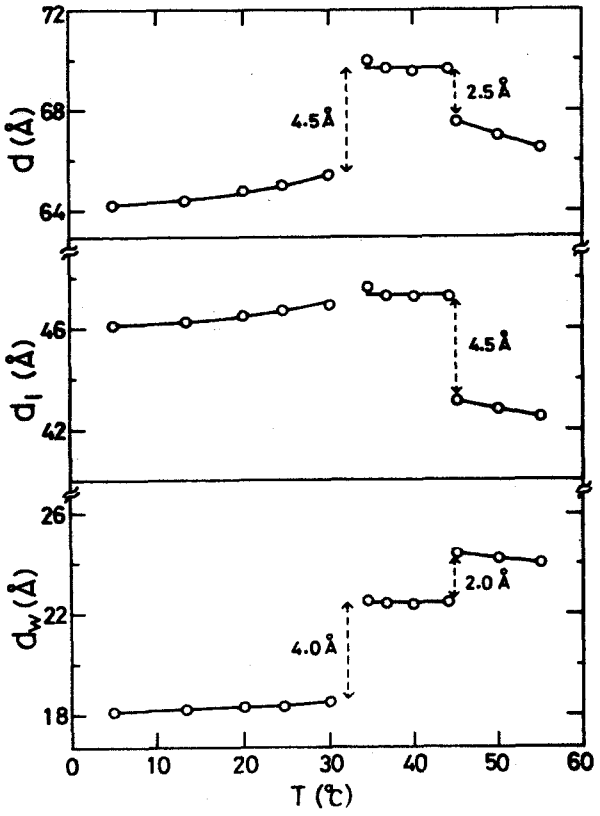

Fig. II-8

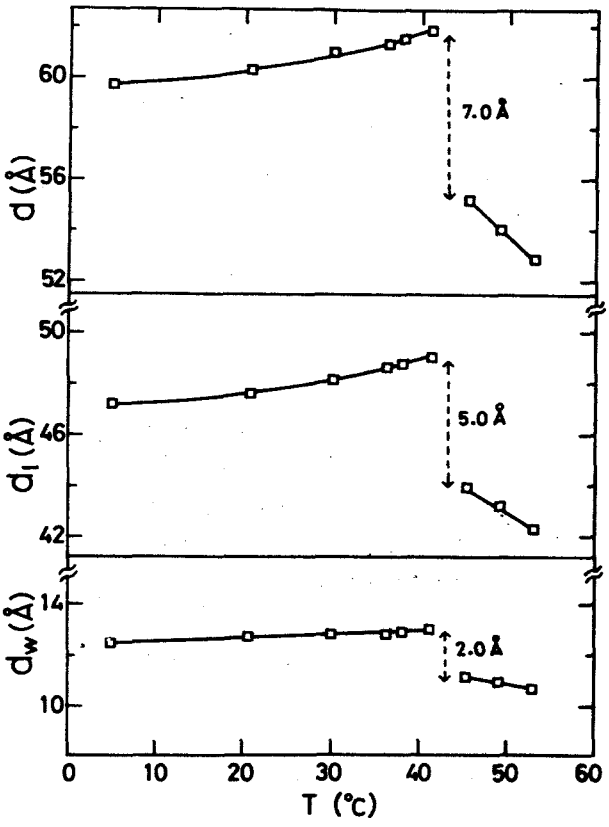

Fig.II-7. Parameters d, d_l and d_w in DPPC lamellar phase in the presence of excess water as functions of temperature T.

Fig.II-8. Parameters d, d_l and d_w in DPPC lamellar phase in the absence of excess water as functions of temperature T. c' = 0.8.

obtained F(Z) in $0.009\,\mathring{A}^{-1} \ll Z < 0.088\,\mathring{A}^{-1}$. $|F(Z)|^2$ calculated with this model are given for $Z < 0.009\,\mathring{A}^{-1}$ in Fig.II-5 in addition to the experimental data for larger angles. These combined data for $0 < Z < 0.088\,\mathring{A}^{-1}$ were used for calculations of $\rho(z)$. They consist of four peaks including the one at $Z = 0$. By the same reasoning as did by Furuya et al. [32], we assigned phases 0, π, 0, π to F(Z) of these four peaks starting from the peak at $Z = 0$. This phase assignment was justified also by the step function model. The electron density projection $\rho(z)$ obtained by the Fourier transform of F(Z) are shown in Fig.II-9 (see Appendix A-5).

II-5 Discussion

Fig.II-7 shows that the thickness d_1 of lipid bilayer does not change appreciably at the pretransition but drops down by about $4.5\,\mathring{A}$ at the main transition. The same tendency can be seen in $\rho(z)$'s shown in Fig.II-9. The two peaks of each $\rho(z)$ [51] indicate the head group positions in lipid bilayer and therefore the peak separation is expected to change in parallel with d_1. We examined validity of this expectation by calculating the Fourier transform of step function models (Appendix A-6). Results assured that the peak separation of calculated $\rho(z)$ is not sensitive to the termination error and changes in parallel to the thicknesses of the model bilayers. The peak separations of $\rho(z)$'s in

Fig. II-9

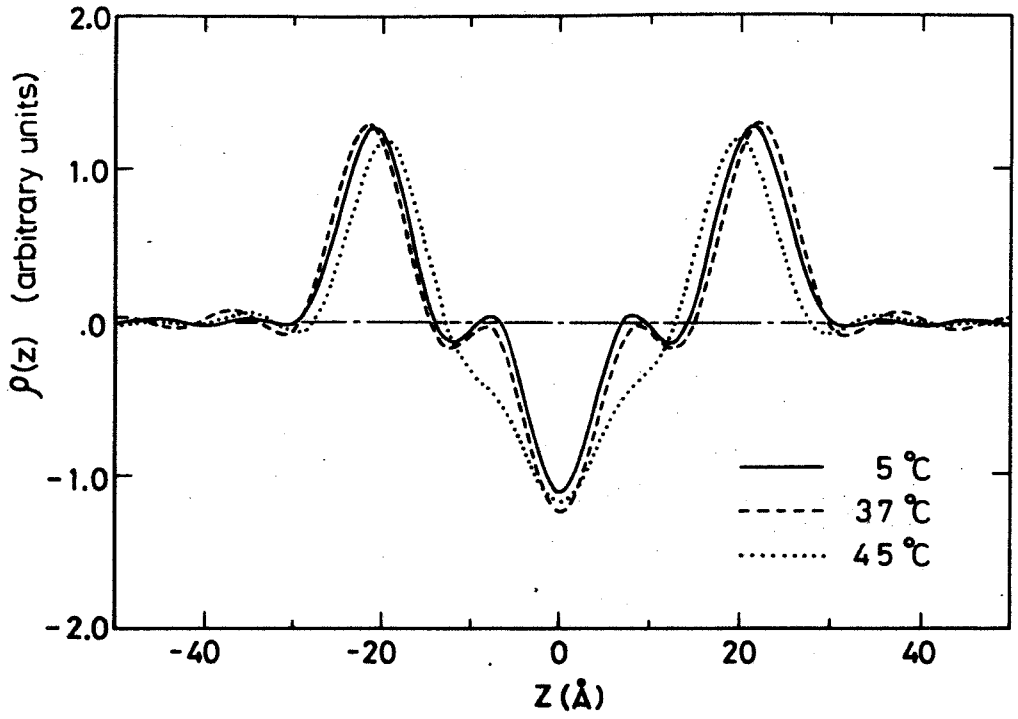

Fig.II-9. Electron density distributions ρ(z) of DPPC bilayer in the presence of excess water at three temperatures. ——— , 5°C; - - - - , 37°C; ....., 45°C.

Table II-2

Best-fit Models of Structures of Lipid Bilayer at Three Temperatures

T (°C)	x_1 (Å)	x_2 (Å)	x_3 (Å)	ρ1	ρ2	ρ3
5	3.0	16.0	26.5	-1.15	-0.09	1.00
37	4.5	17.0	26.5	-1.00	-0.09	1.00
45	6.0	14.5	25.0	-1.05	-0.28	1.00

parameters ρ_1, ρ_2, ρ_3 and x_1, x_2, x_3 are the density levels in a relative scale and the extensions of the terminal methyl trough, hydrocarbon core and polar head group, respectively.

Fig.II-9 are 42 Å at 5°C, 43.5 Å at 37°C and 39 Å at 45°C. These values suggest that d_l will increase by about 1.5 Å from 5°C to 37°C and decrease by about 4.5 Å from 37°C to 45°C, in good agreement with the changes in d_l in Fig.II-7. These results prove that the d_l and d_w curves in Fig.II-7 are reasonablly reliable although they were obtained on the assumption that c is constant in each of the three phases. Fig.4b of the paper by Janiak et al. [43] gave data of d vs. (1-c') for DPPC at 39°C, giving $c^* = 0.25$ and $d^* = 65.6$Å. This value of d^* is quite different from ours (69.5 Å at 37°C), and also from that observed by Rand et al. [42] in the presence of excess water (70 Å for 36 ∼ 41°C). We repeated experiments and found our results reproducible.

Before starting this study the temperature dependence of d in the presence of excess water (Figs II-1 and 7) was puzzling because of the following two reasons. Firstly the discontinuous change of d at the pretransition is larger than at the main transition whereas anomalies of other physical quantities (e.g., the specific heat) are much smaller at the pretransition than at the main transition. Secondly, d is larger in the intermediate phase between the two transition points than in the lower- and higher-temperature phases, whereas x-ray diffraction patterns [5,42-44] suggested that degree of disorder in the arrangement of hydrocarbon chains of lipid increases at each transition temperature with rising temperature. Now the behaviours of

d have been made more understandable by decomposing it into d_l and d_w as shown in Fig.II-7. The variation of d_l seems to be in accordance with changes of other physical quantities at the pre- and main transitions. It seems reasonable to expect that the thickness d_w of water is more closely related with arrangements of the head groups of lipid than with the hydrocarbon chains. The variation of d_w seems to suggest that the pretransition is associated with some rearrangement of the head groups of lipid. According to Salsbuly et al. [52], deuterium NMR spectra indicated that there is a modification in the arrangement of water molecules around the head group at the pretransition.

Another puzzling fact was that the discontinuous change of d at the main transition was more distinct in the absence of excess water as seen in Fig.II-1a. Now it has become more understandable because d_w jumps up at the transition in the presence of excess water (Fig.II-7) but drops down in the absence of excess water (Fig.II-8) whereas d_l changes by about the same amount both in the presence and the absence of excess water.

Egg-yolk lecithin bilayers assume the Lα phase at room temperatures and large d_w values were reported for the lamellar phase in water (e.g., 27.5 Å at about 25°C [16]). This value is much larger than d_w of 18.5 Å at 25°C in Fig.II-7, but extrapolation of the d_w vs. T curve of the Lα phase in Fig.II-7 gives d_w as about 25 Å. Therefore,

presumably the larger value of d_w is not characteristic to egg-yolk lecithin but to the Lα phases in general.

Recent studies by LeNeveu et al. [16] and by Ohshima et al. [15] indicated that d_w in pure water is equal to twice the thickness of hydration layer on the lipid bilayer. Therefore, the curve d_w in Fig.II-7 simultaneously demonstrates how the hydration layer changes associated with the phase transitions.

Chapman et al. [5] observed the small anomaly of specific heat around 35°C also for wet specimens of $c' > c^*$, proving that there still exists the pretransition in the absence of excess water. We could not detect any anomaly of d at the pretransition for the specimens of $c' > c^*$ as shown in Fig.II-1a and thus there appear no anomalies in the d_l and d_w curves around 35°C in Fig.II-8. Combining these results with the d_l vs. T curve in Fig.II-7, we may conclude that the thickness of bilayer does not change appreciably at the pretransition irrespective of the presence or absence of excess water. Rand et al. [42] tried to explain the increase of d at the pretransition as caused by a change of tilting angle of the hydrocarbon chains. Their argument was implicitly based upon the postulation that d_l behaves in parallel to d. This was denied by the results in Fig.II-7 and presumably their model should be discarded.

Janiak et al. [43] reported that the additional reflec-

tions characteristic to the Pβ" phase were observed even for $c' < c^*$. We observed the reflections for $c' > c^*$ but not for $c' < c^*$. Therefore, there is a doubt that the intermediate phase is of the Pβ' type in the presence of excess water.

Generally the phase of DPPC bilayer below 35°C is regarded as Lβ'. But probably it should be mentioned here that weak but sharp satellite scatterings appear around the ordinary reflections of the Lβ' phase on X-ray photographs taken with long exposure below 35°C [53] as cited in the ref.54.

As reported before [45], DPPC bilayers exhibit three high-angle reflections at 4.2, 4.1 and 4.0 Å in the aqueous solution of 1 M $CaCl_2$. We observed a somewhat more complicated diffraction pattern for DMPC bilayers. Therefore, the structures of bilayers are different in the solution of 1 M $CaCl_2$ from those in pure water. These diffraction patterns of DPPC and DMPC remained unchanged up to the main transition temperatures indicated by the peaks of d in Figs II-3a and b, respectively. Above these transition temperatures, the patterns gave the broad peak at 4.6 Å, the characteristic feature of the Lα phase. These results are in accordance with the observations by Chapman et al. [55] that there was no specific heat anomaly characteristic to the pretransition in DMPC bilayers in solution of 1 M $CaCl_2$. The repeat distance d itself does not change discontinuously

at the main transition in Fig.II-3 unlike the data in Fig.II-1, suggesting the possibility that the mechanism of the transition is somehow different from in pure water.

II-6 Summary

(1) In both cases of the presence and the absence of excess water, the thickness d_l of the lipid bilayer of DPPC lamellar phase does not change appreciably at the pretransition (35°C) but drops down by about 5 Å at the main transition (42°C) with increasing temperature.

(2) In the presence of excess water, the thickness d_w of the water layer between bilayers jumps up by 4.0 Å at the pretransition and by 2.0 Å at the main transition.

(3) In the absence of excess water, d_w does not change at the pretransition but drops down by about 2.0 Å at the main transition.

(4) These results prove that there is practically no change of the tilting angle of hydrocarbon chains at the pretransition and that the remarkable increase of the repeat distance d of the lamellar phase at the pretransition in the presence of excess water is caused by the increase in d_w.

CHAPTER III

X-RAY DIFFRACTION STUDIES OF DIPALMITOYL PHOSPHATIDYL-CHOLINE - PROTEIN COMPLEXES WITH SPECIAL REFERENCE TO CYTOCHROME b_5

III-1 Introduction

There are many works on lipid-protein complexes as surveyed by Shipley [56]. To our knowledge, however, studies have been limited so far to complexes of positively charged non-membrane proteins and negatively charged lipids. Our recent studies [45] have suggested that addition of $CaCl_2$ to dipalmitoyl phosphatidylcholine-water system produces positively charged lipid bilayers. They are dispersed without forming lamellar structures in aqueous solution of 5 mM $CaCl_2$ [45] (see Chapter I). Utilizing these facts, we have succeeded in producing lamellar structures made of negatively charged proteins and the bilayers. Proteins examined were the membrane protein cytochrome b_5 and three non-membrane proteins (albumin, ovalbumin and β-lactoglobulin A). X-ray observations on structures of the lamellar phases and modes of lipid-protein bindings are reported below

III-2 Materials and Methods

Synthetic β, γ-dipalmitoyl-D,L-(α)- phosphatidylcholine (DPPC) was purchased from Sigma Chemical Co., and used without further purification. It was stored at-20°C in chloroform at the concentration of 2 mM. Cytochrome b_5 was extracted from rabbit liver microsomes by using Triton X-100, and purified following the method described by Spatz and Strittmatter [57]. The detergent was eliminated by dialysis and a Sephadex G-25 column. Cytochrome b_5 obtained in this way will be abbreviated as d-b_5 below. The hydrophilic portions of d-b_5 which contain the heme were obtained by the trypsin action in the same manner as described by Dufourcq et al. [58]. After gel filtration on Sephadex G-100 column, the collected fractions of the hydrophilic portions were concentrated by means of ultra filtration. This trypsin-treated cytochrome b_5 is abbreviated as t-b_5 below.

Albumin (bovine serum,crystallized), ovalbumin (Grade II) and β-lactoglobulin A (milk) were obtained from Sigma Chemical Co.. The d-b_5 and t-b_5 were stored below -20°C in 20 mM Tris-acetate buffer, PH 8.1. The other proteins were stored at about 0°C in powder.

DPPC was suspended in 10 mM Tris-acetate buffer, PH 8.1, containing 5 mM $CaCl_2$. As reported before [45], in the presence of small amount of $CaCl_2$, DPPC bilayers are dispersed uniformly in aqueous solution without forming lamellar structure. Lipid-protein complexes were prepared by incubating such suspension of DPPC bilayers with d-b_5, t-b_5

or other proteins. Incubation was done at 0 ∿ 45°C for 30 min ∿ 20 h. The weight ratio of protein/lipid in mixture was approximately 0.2/1 ∿ 1/1. The content of d-b_5 and t-b_5 were estimated from the absorbance at 413 nm (extinction coefficient $\varepsilon = 117\ mM^{-1}cm^{-1}$), and the contents of other proteins were determined by the method of Lowry et al. [59].

Samples were sealed in thin-walled X-ray glass capillaries having 1.0 mm internal diameter. Then they were centrifuged at 20 000 × g for 30 min by holding the capillary in the hole of a modified centrifuge tube to obtain densed specimens.

X-ray diffraction patterns were recorded photographically on an Elliott toroidal focusing camera using Ni-filtered Cu Kα radiation ($\lambda = 1.542$ Å) from a Rigaku Denki rotating anode microfocus generator. Exposure time was 6 ∿ 20 h. Samples were maintained at about 5°C during X-ray measurements. Optical densities of the films were measured by a microdensitometer. Non-linearity between X-ray intensity and optical density was corrected by a standard scale.

Fig.III-1. Low-angle diffraction photographs of d-b_5-DPPC and t-b_5-DPPC complexes. (a) Pattern from d-b_5-DPPC complex incubated above 35°C. Repeat distance d is 114 Å. (b) Pattern from d-b_5-DPPC complex incubated below 35°C, d = 150 Å. (c) Pattern from t-b_5-DPPC complex incubated at 0°C (or 38°C), d = 100 Å.

Fig. III-1

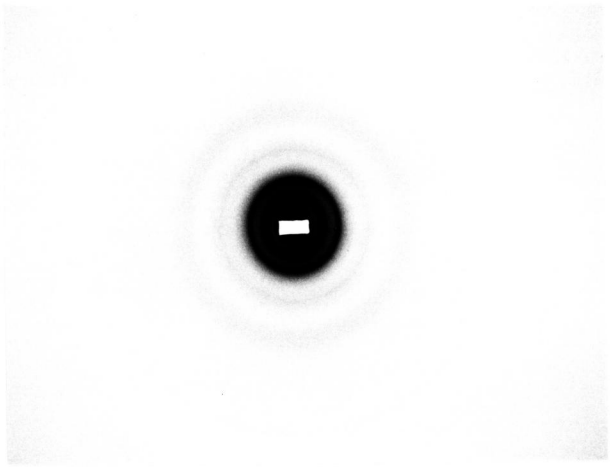

a

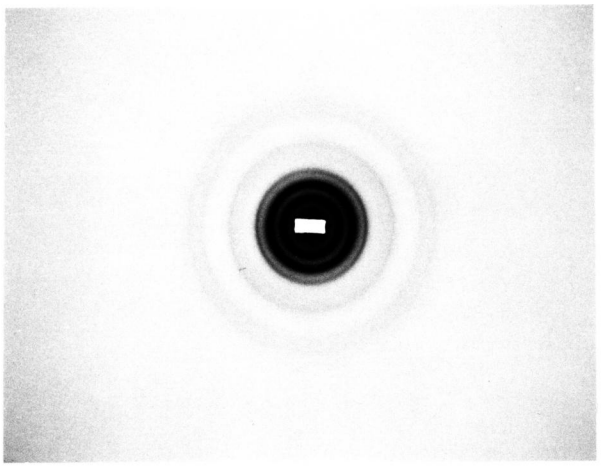

b

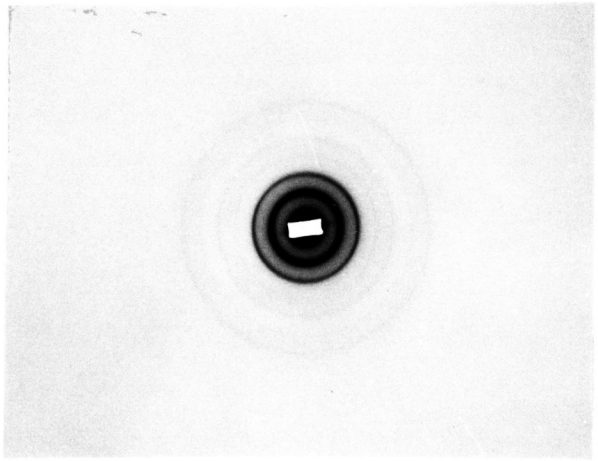

c

III-3 Results

Formation of lipid-protein lamellar phases

Complexes of DPPC and cytochrome b_5 or three non-membrane proteins were subjected to X-ray diffraction measurements.

A set of diffraction lines were observed in the low-angle region of photographs for all complexes. These reflections can be indexed as integral orders of one-dimensional repeat, suggesting the production of the lamellar phase between these proteins and DPPC bilayers. Fig.III-1 shows X-ray diffraction photographs from three types of the complexes with cytochrome b_5.

Fig.III-2 gives a plot of the measured repeat distance versus the cube root of the molecular weight of the component protein for each complex. Among four proteins except the d-b_5, there is a linearity between the repeat distance and cube root of the molecular weight. The d-b_5-DPPC complexes seem to be off this relationship. As shown in Fig.III-2, the d-b_5 forms two types of lamellar phases with repeat distances of 114 Å and 150 Å depending upon the incubation temperature. The former lamellar phase was obtained when the complex was incubated above 35°C, while the latter was obtained when incubated below 35°C. This critical temperature 35°C coincides with the pretransition point of DPPC bilayer. In the cases of t-b_5 and non-membrane proteins,

Fig. III-2

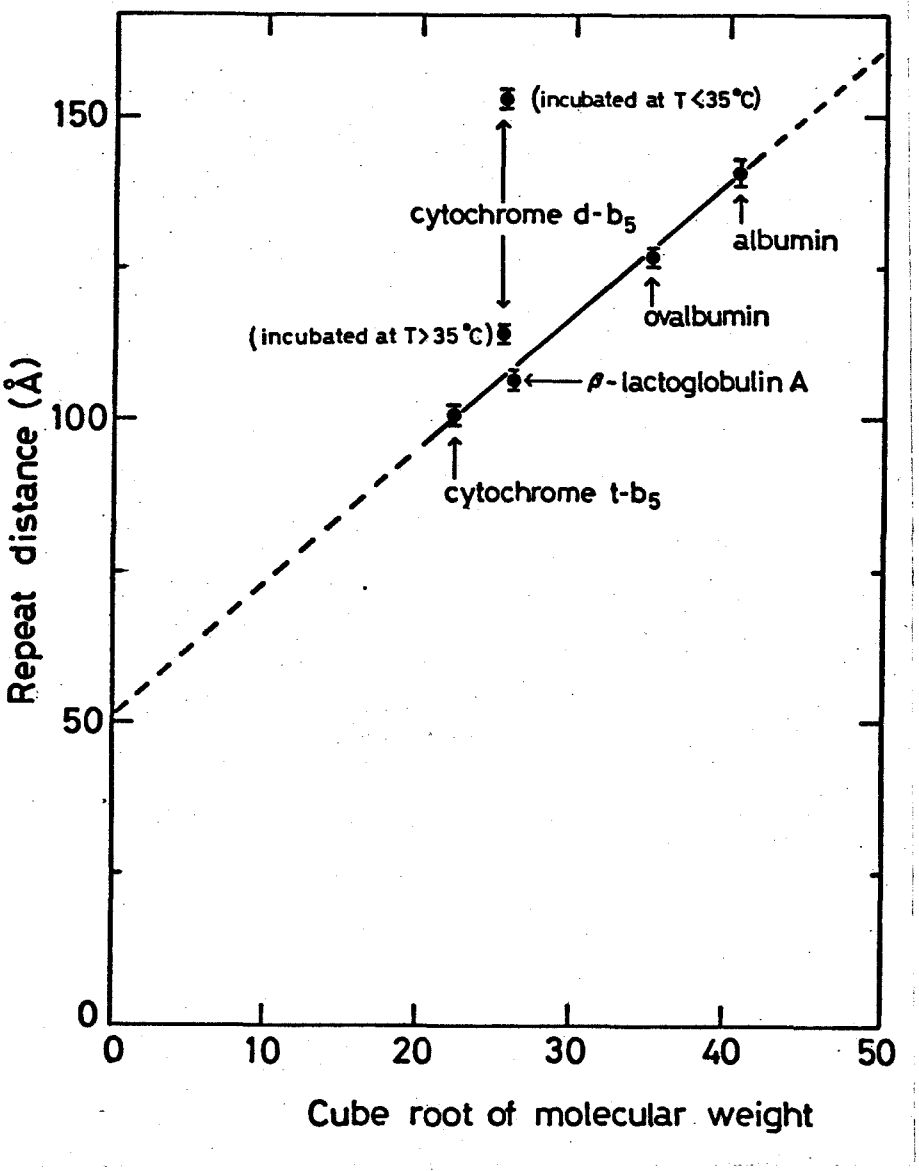

Fig.III-2. A plot of the repeat distance vs. the cube root of the molecular weight of component protein for six DPPC-protein lamellar phases. β-lactoglobulin A dissociates into half-molecules under the condition of the experiments [60].

the repeat distances of their lamellar phases were not independent of the incubation temperature and were constant, respectively.

Hydrophobic and electrostatic interactions between protein and lipid

Fig.III-3 illustrates profiles of the high-angle peaks for some complexes. Curves 1 and 2 are for d-b_5-DPPC complexes incubated above and below 35°C, respectively. Curve 3 is for t-b_5-DPPC complex. Curve 4 is for pure DPPC bilayers and shows a pattern typical of the Lβ' phase.[14]. As compared with Curve 4 , Curves 2 and 3 show no detectable changes in their profiles. The similar results were obtained for three non-membrane proteins. These complexes were dissociated in lipid and protein by adding electrolytes (0.5 M NaCl, 0.5 M KCl) or EDTA (10 mM), and consequently pure DPPC lamellar phase with a repeat distance of about 65 Å was reproduced.

In contrary with this, Curve 1 gives a slight diffuse reflection at about 4.2 Å. This indicates that the order array of the hydrocarbon chains in DPPC bilayers in the gel state were disturbed by the penetration of the hydrophobic "tail" of d-b_5. Such high-angle profile was not affected with addition of electrolytes or EDTA. X-ray diffraction patterns, however, revealed that after treatments the complexe does not form the lamellar phase and

Fig. III-3

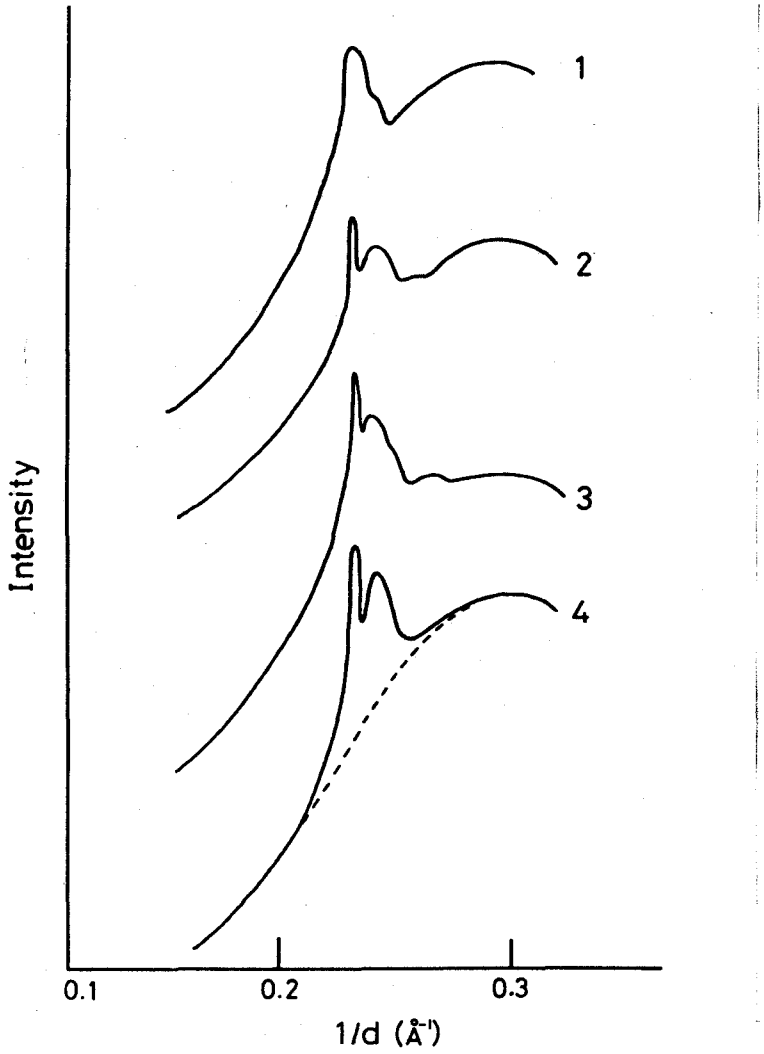

Fig.III-3. High-angle reflection profiles of cytochrome b_5-DPPC and pure DPPC lamellar phases. Curve 1, d-b_5-DPPC lamellar phase incubated above 35°C; Curve 2, d-b_5-DPPC lamellar phase incubated below 35°C; Curve 3, t-b_5-DPPC lamellar phase incubated at 0°C (or 38°C); Curve 4, pure lamellar phase.

dissociates in single bilayers bearing d-b_5. These observations suggest the hydrophobic interaction between the d-b_5 and DPPC bilayers.

Electron density profile of d-b_5-DPPC membrane

Fig.III-4 shows the Fourier syntheses for the electron density distributions $\rho(z)$ across d-b_5-DPPC membrane and pure DPPC bilayer. The $\rho(z)$ of d-b_5-DPPC membrane was calculated using the first eight reflections observed, and that of pure DPPC bilayer using the reflections up to 8th order obtained by the sampling of the continuous intensity curve of DPPC bilayer (see Fig.II-5 in Chapter II) at a interval of 1/114 $\mathring{A}^{-1}$. The intensities of these reflections are listed in Table III-1. The phases of reflections for each case were determined from the continuous diffraction pattern of single d-b_5-DPPC membrane or DPPC bilayer (see Appendix A-5).

As compared with the profile of DPPC bilayer, the profile of d-b_5-DPPC membrane shows a slight increase in the peak separation and also the rise of electron density on the outside of the head group region. This increase in electron density probably originates from the hydrophilic portions of d-b_5 which are distributed on the bilayer surface. The molar ratio of lipid and protein in this membrane was approximately 30/1.

Fig.III-4

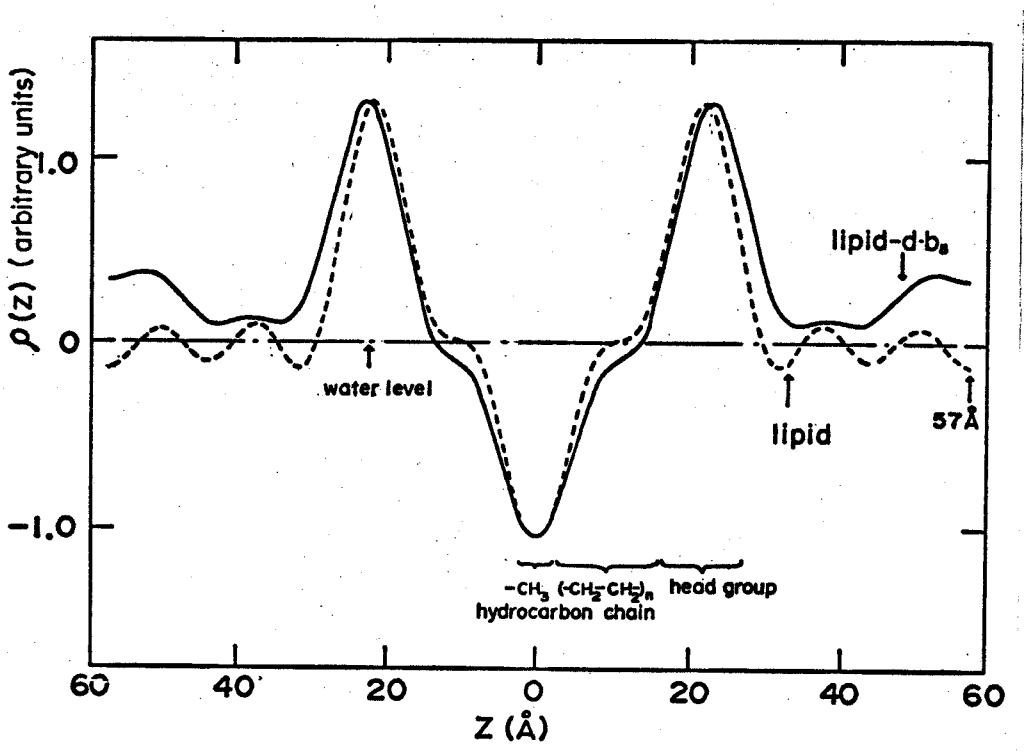

Fig.III-4. Electron density distributions of d-b_5-DPPC membrane and of pure DPPC bilayer as reference. ———, d-b_5-DPPC membrane, phase choice (π, π, π, π, 0, 0, π, π); — — — — , pure DPPC bilayer, phase choice (0, π, π, π, 0, 0, π, π).

Table III-1

Intensity Data for Lamellar Reflections

h	d-b_5-DPPC membrane	DPPC bilayer
1	5.1	∿0
2	37.5	36.3
3	43.9	42.7
4	∿0	3.6
5	4.0	4.2
6	∿0	0.8
7	3.7	3.9
8	3.0	8.6

III-4 Discussion

The low-angle diffraction data on the complexes of DPPC bilayers and d-b_5, t-b_5 and non-membrane proteins (albumin, ovalbumin and β-lactoglobulin A) revealed the formation of the lamellar structure between them. As reported before [45], DPPC bilayers are positively charged by bound Ca^{2+} in the aqueous solution containing $CaCl_2$. On the other hand, all the proteins examined have isoelectric points of less than 7.0. They are, hence, negatively charged in the buffer solution with PH of 8.1. Therefore, under these conditions, these proteins and DPPC bilayers mixed together probably associate by electrostatic interaction and make the lamellar phases.

The measured repeat distances of these lamellar phases (Fig.III-2) suggest that two layers of protein molecules are inserted between DPPC bilayers. This model is supported by the fact that the remainder of each repeat distance which is subtracted by the bilayer thickness (46 ∿ 48 Å [5,14,61]) corresponds to the twofold dimension of each protein [62-65]. The linearity between the observed repeat distance and the cube root of the molecular weight may be explained by an idea that the sizes of these proteins are nearly propotional to the cube roots of the molecular weight because of their globular shapes. Moreover, an intercept of the straight line in Fig.III-2 on the left vertical axis gives the partial

thickness of DPPC bilayer in the lipid-protein lamellar phase. The result of about 50 Å is in good agreement with the reported value of 46 ∿48 Å [5,14,61].

The results on cytochrome b_5 -DPPC complexes showed some modes concerning the interaction of them. The high-angle reflection profiles (Fig.III-3) suggested that the interaction of t-b_5 and DPPC bilayers is electrostatic in nature and that the binding of d-b_5 to DPPC bilayers is at least partly hydrophobic when incubated above 35°C. If the d-b_5 interacts with DPPC bilayers by embedding the whole of its hydrophobic tail into the bilayers, the repeat distance of this lamellar phase should nearly equal that of t-b_5-DPPC lamellar phase. However, the former gives a larger repeat distance than the latter; there is a difference of about 14 Å between them, as seen in Fig.III-2. Part of this increase is probably caused by the increase in the thickness of the bilayer. This was supported by the fact that the electron density profile of d-b_5-DPPC membrane in Fig.III-4 shows increase of about 3 Å in the peak separation. Also, it was reported that the thickness of DPPC bilayer is increased by the penetration of the "foreign" molecules e.g., cholesterol [9,21]. However, a increase of 14 Å can not be perfectly complemented by this change (∿ 3 Å). These results therefore imply that a part of the hydrophobic segment emerges from the surface of bilayer into the water.

When the d-b_5 and DPPC bilayers were incubated below

35°C, they made the lamellar structure with a repeat distance of 150 Å. In this case, however, the d-b_5 can not get into the bilayer and seems to adsorb on the bilayer surface. It is known that the d-b_5 self-associates in an aqueous solution and exists as a oligomer [57,62,66,67]. Also, the molecular weight of this oligomer has been reported to be $1 \times 10^5 \sim 1.4 \times 10^5$ [57,62,66,67], suggesting octamer. Therefore, from these facts, it is suggested that the oligomes of d-b_5 are sandwiched between bilayers without dissociating in monomer when the complex is incubated below 35°C. Similar results were observed with dimyristoyl phosphatidylcholine (DMPC). In this case, the critical incubation temperature was nearly the pretransition point of 11°C [5,41] of this lipid bilayer.

Thus, it was found that the d-b_5-DPPC complex two types of interaction depending upon the incubation temperature. This cause is likely to be sought in the difference of the bilayer structure during incubation. That is, the the hydrocarbon chains in the flat DPPC bilayer are rigid [5, 42-44] below the pretransition point, but become partially disorder [5,42-44] in the intermediate phase between the pre- and main transition points. Recently, Faucon et al. [68] observed in fluoresence polarization study that the interaction of DPPC vesicles with the d-b_5 occurs below the pretransition temperature (at 20°C). However, we observed on the high-angle diffraction pattern of small

DPPC vesicles that the hydrocarbon chains are rather disordered. In this respect our results do not contradict with their results.

Our x-ray observations on d-b_5-DPPC complexes suggest that the conformational state of the hydrocarbon chains in lipid bilayer is closely connected with the ability of binding of the d-b_5 to lipid bilayers.

III-5 Summary

(1) It has been succeeded in producing lamellar phases of negatively charged proteins and DPPC bilayer. The proteins used were the membrane protein cytochrome b_5 from rabbit liver and three non-membrane proteins (albumin, ovalbumin and β-lactoglobulin A).

(2) Detergent-extracted cytochrome b_5 forms two types of lamellar phases with DPPC, depending upon the incubation temperature. The repeat distance is 114 Å when incubated above 35°C and is 150 Å below 35°C. The critical temperature 35°C coincides with the pretransition point of DPPC bilayer.

(3) X-ray diffraction patterns suggested that the binding of detergent-extracted cytochrome b_5 to DPPC bilayer is hydrophobic above 35°C and electrostatic below 35°C, and that binding of trypsin-treated cytochrome b_5 and the above-mentioned three non-membrane proteins to DPPC bilayer are electrostatic when incubated at 0°C and 38°C.

APPENDIX

A-1 Symbols and Abbreviations

Phospholipids

DPPC	dipalmitoyl phosphatidylcholine
DMPC	dimyristoyl phosphatidylcholine

Structure of the phases

L	one-dimensional lamellar
P	two-dimensional oblique or rectangular
α	hydrocarbon chains are in liquid-like with the average of the chain orientations perpendicular to the bilayer plane
β	chains are stiff and parallel, oriented at right angles to the bilayer plane and packed with rotational disorder in a two-dimensional hexagonal lattice
β'	similar to β, but with the chains tilted with respect to the normal to the bilayer plane

Structural parameters

N_o	Avogadro number
M	molecular weight of lipid
$\bar{v}_l$ and $\bar{v}_w$	partial specific volumes ($cm^3 g^{-1}$) of lipid and water
c	weight ratio of lipid (lipid/(lipid + water)) in the lamellar phase
$c_v = \frac{c\bar{v}_l}{c\bar{v}_l + (1-c)\bar{v}_w}$	volume ratio of lipid in the lamellar phase
d	repeat distance (Å) of the lamellar phase
$d_l = c_v d$	partial thickness (Å) of the uniform lipid layer of one unit of the lamellar phase
$d_w = (1-c_v) d$	partial thickness (Å) of the water layer
$S = \frac{2M\bar{v}_l}{N_o d_l}$	average area ($Å^2$) per one lipid molecule on the lipid-water interface

A-2 Constitutional Formulae of Lipids Used

Fig.A-1 shows the constitutional formulae of the lipids used in the present studies.

Fig. A-1

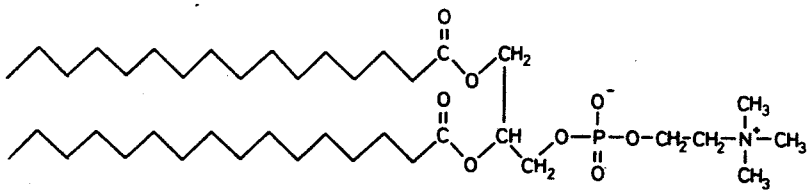

(a) Dipalmitoyl phosphatidylcholine (DPPC)

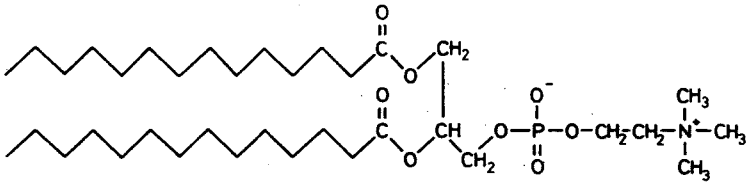

(b) Dimyristoyl phosphatidylcholine (DMPC)

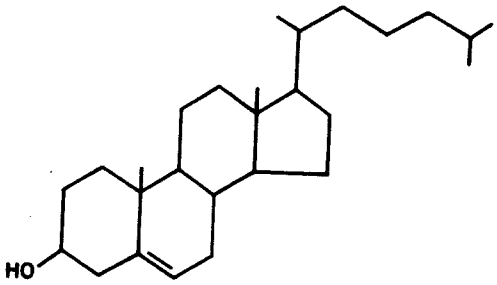

(c) Cholesterol

Fig.A-1. Constitutional formulae of the three lipids used. (a) dipalmitoyl phosphatidylcholine. (b) Dimyristoyl phosphatidylcholine. (c) Cholesterol.

Fig. A-2

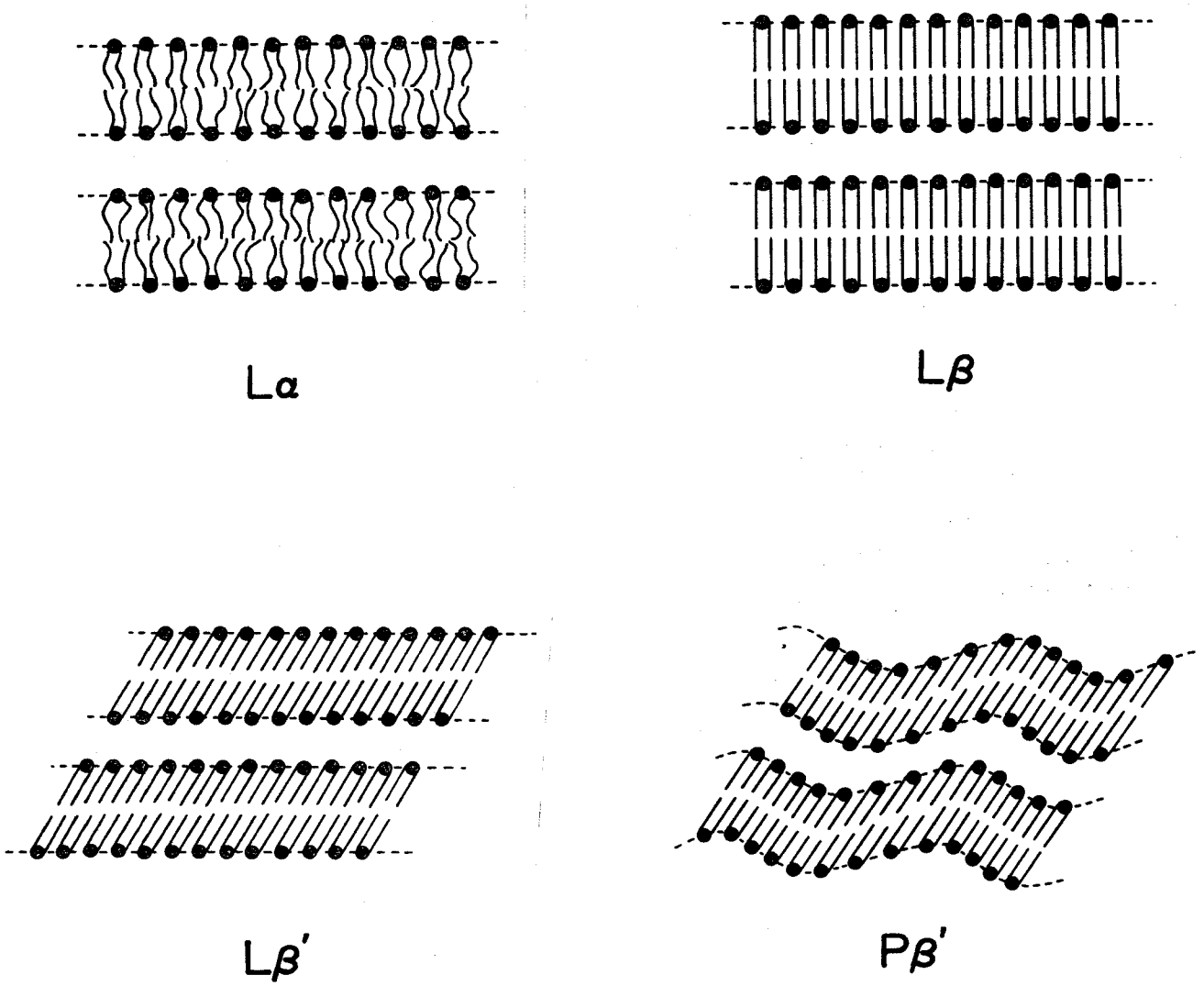

Fig.A-2. Schematic representations of the four phases in the lamellar structure. (a) Lα phase. (b) Lβ phase. (c) Lβ' phase. (d) Pβ' phase. (For definition of these symbols, see Appendix A-1.)

A-3 Illustration of Four Phases of Lecithin Bilayers

The phases appearing in the phosphatidylcholine-water systems are designated according to the nomenclatures of Luzzati et al. [6] and Tardieu et al. [14].

Fig.A-2 gives schematic representations of the four phases, Lα, Lβ, Lβ' and Pβ' discussed in this thesis. All these phases are belong to the lamellar class. The capital Latin letter in each symbol specifies the type of lattice and the Greek letter defines the conformation of the hydrocarbon chains (see Appendix A-1).

A-4 X-ray Optics Used

Fig.A-3 shows optical arrangements of two types of focusing cameras used in the present studies and of pinhole camera. Focusing cameras collect a divergent beam of radiation from the source and concentrate it into a fine spot by the total reflection from a pair of curved mirrors (Fig.A-3b) or from a toroidal reflector (Fig.A-3c). Therefore, the focusing cameras give greater intensities than the pinhole camera (Fig.A-3a) in which a narrow beam of X-rays is defined by a pair of circular apertures. Using these focusing cameras with a rotating anode X-ray generator, we can shorten the exposure time and obtain more distinct diffraction patterns on low backgrounds.

Fig. A-3

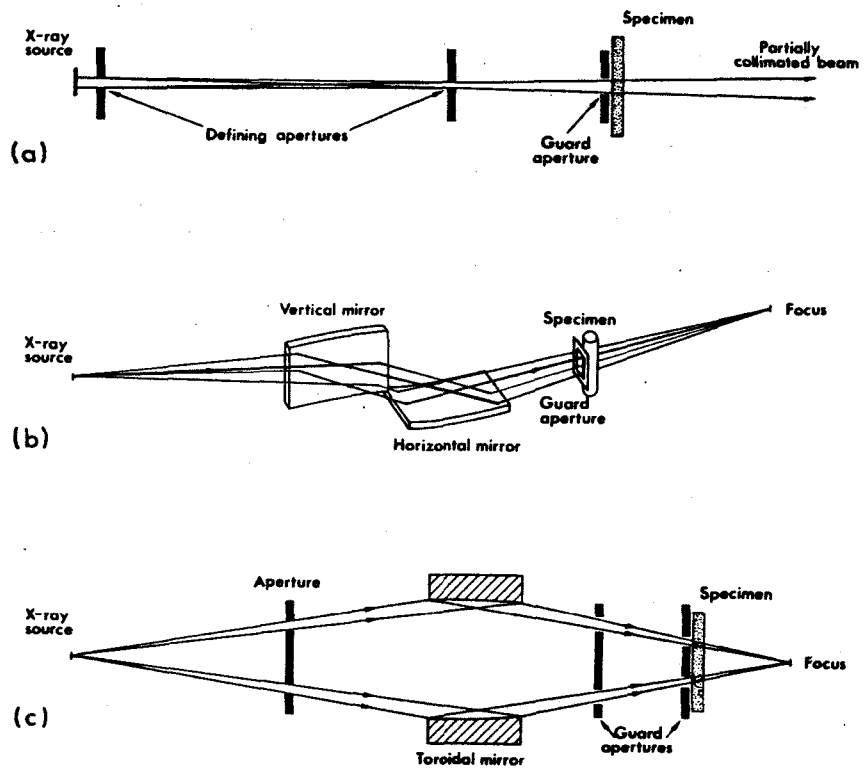

Fig.A-3. Optical arrangements used to obtain X-ray diffraction patterns. (a) Pinhole Collimation [69]. (b) Focusing mirror system using elastically deformed optical flats [70, 71]. A similar arrangements is used with curved-crystal monochromators except that the reflectors are oriented so that the central ray lies in a principal plane of the surface. (c) Focusing mirror system using a toroidal reflector [72] and annular apertures.

A-5 Calculations of Electron Density Distributions in Bilayers

Let us consider the system in which single bilayers are dispersed. There exists the following relationship between the observed intensities, I(Z) and the scattering amplitude, F(Z).

$$|F(Z)|^2 = Z^2 I(Z) \qquad \text{(A-1)}$$

where Z is the reciprocal coordinate perpendicular to the bilayer, related to the scattering angle 2θ by $Z = 2\sin\theta/\lambda$. A correction factor of Z in Eqn.A-1 arises from the geometrical arrangement of the specimen and a second factor of Z from the divergence of X-ray beam.

We can obtain the electron density distribution $\rho(z)$ projected onto the normal (z-coordinate) to lipid bilayer by the inverse Fourier transform of F(Z). That is,

$$\rho(z) = \int_{-Z_{max}}^{Z_{max}} F(Z)\, e^{-2\pi i z Z}\, dZ \qquad \text{(A-2)}$$

Here, we must determine the phase of F(Z) in order to obtain F(Z) from the corrected intensity $|F(Z)|^2$. For a centro-symmetric structure such as lipid bilayer, the phase problem is reduced to the choice between two possible angles, 0 and π. We assigned the phases 0, π, 0, π to F(Z) of the first four peaks starting from the peak at Z = 0, assuming

that F(Z) changes its sign at each zero points of $|F(Z)|^2$. This assumption is based on the principle of minumal wavelength by Bragg and Perutz [73]. Also, many experimental studies of lipid bilayers supported the phase combination of (0, π, 0, π) for F(Z) of the first four peaks [31,74-76].

In the case of the systems containing the lamellar phase, F(Z) and I(Z) respectively are replaced by F(h) and I(h), where h is the order of the lamellar reflection. For Eqns A-1 and 2, we have

$$|F(h)|^2 = h^2 I(h) \qquad \text{(A-3)}$$

$$\rho(z) = \frac{2}{d} \sum_{h=1}^{h_{max}} F(h) \cos(2\pi z h/d) \qquad \text{(A-4)}$$

where d is the length of one-dimensional repeat distance. Values of $|F(h)|^2$ is propotional to $|F(Z)|^2$ at $Z = h/d$. In this case, the phases of the reflections can not be determined directly. However, if the continuous scattering intensity $|F(Z)|^2$ is obtained independently, we can assign the phase of each reflection from the relationship between the reciprocal lattice position of the reflection and the peaks of F(Z).

A-6 Reliability of Peak Separation of Calculated $\rho(z)$ as a Measure of Bilayer Thickness

We examined the validity of the comparison among the

Fig. A-4

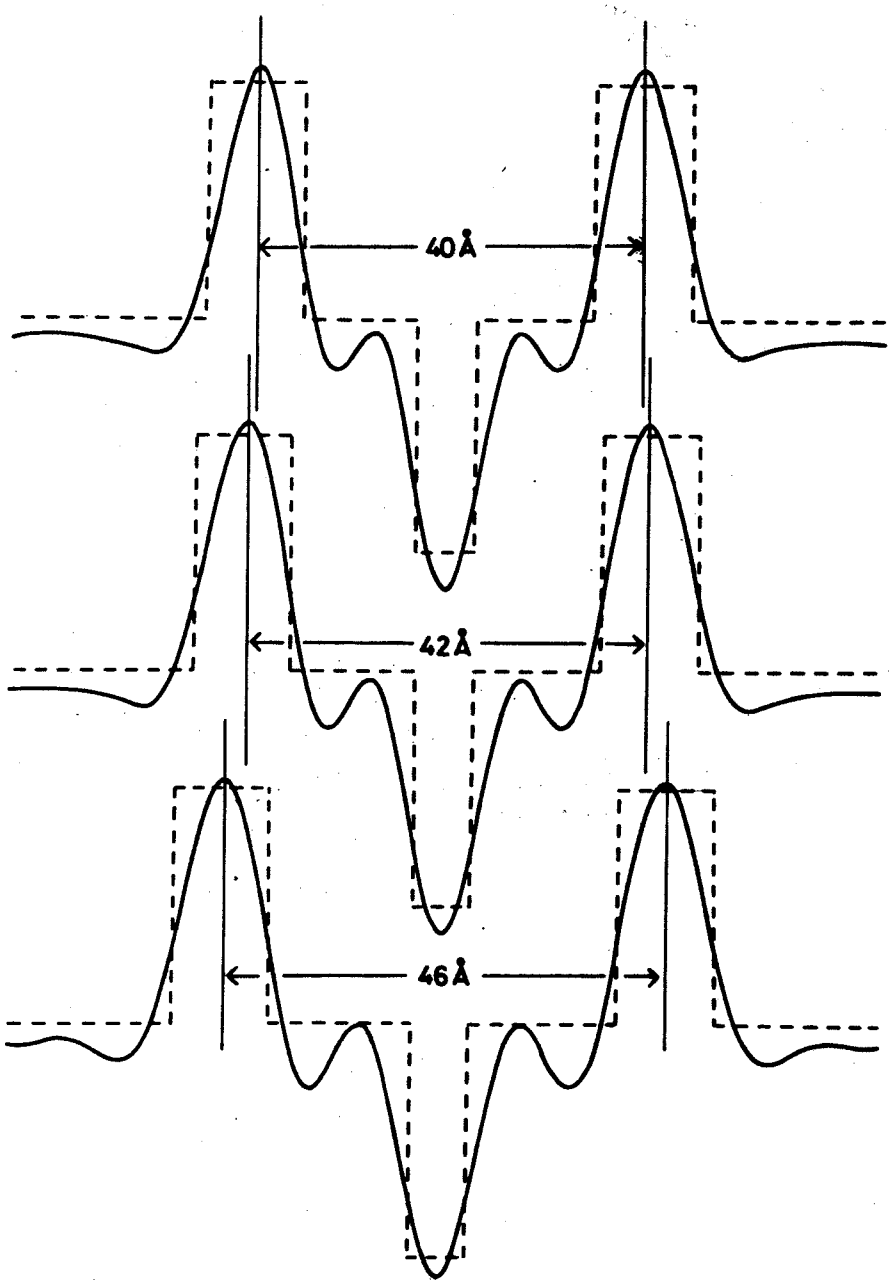

Fig.A-4. Three step function models with different peak separations and the rebuilt profiles calculated by the Fourier - inverse Fourier transforms. - - - - , Step function models; ——— , rebuilt profiles.

profiles of lipid bilayer calculated to the same and lower resolution ($\sim$11 Å). The three dotted lines in Fig.A-4 represent the step function.models with the peak separations of 40, 42 and 46 Å, respectively. We calculated the Fourier transform of each model in the range of $0.009\ \text{Å}^{-1} < Z < 0.088\ \text{Å}^{-1}$. Using these computed data, we rebuilt the density distributions of the original models. The results are shown by the solid curves in Fig.A-4. As can be seen from Fig.A-4, the peak separation of the rebuilt profile changes in parallel with that of the step function model, and the peak positions are reproduced exactly. Therefore, these results assure that the peak separations of $\rho(z)$ given in Fig.II-9 are very reliable in the values.

ACKNOWLEDGEMENTS

I wish to express my appreciation to Prof. T. Mitsui for many variable discussions and his encouragements throughout this study. I also thank Dr. T. Ueki for many helpful discussions and Dr. H. Nakamura for many technical advices on preparing cytochrome b_5. I have benefited greatly from the discussions and suggestions offered by other members in this laboratory.

REFERENCES

1. Luzzati,V., Mustacchi,H. and Skoulios,A.E. (1957) Nature 180, 600-601
2. Luzzati,V. (1968) in Biological Membranes (Chapman, D.,ed.), Vol 1, p.71-123, Academic Press, London
3. Luzzati,V. and Husson,F. (1962) J. Cell Biol. 12, 207-219
4. Reiss-Husson,F. (1967) J. Mol. Biol. 25, 363-382
5. Chapman,D., Williams,R.M. and Ladbrooke,B.D. (1967) Chem. Phys. Lipids 1, 445-475
6. Luzzati,V., Gulik-Krzywicki,T. and Tardieu,A. (1968) Nature 218, 1031-1034
7. Small,D.M., Bourges,M.C. and Dervichian,D.G. (1966) Biochim. Biophys. Acta 125, 563-580
8. Bourges,M.C., Small,D.M. and Dervichian,D.G. (1967) Biochim. Biophys. Acta 137, 157-167
9. Ladbrooke,B.D., Williams,R.M. and Chapman,D. (1968) Biochim. Biophys. Acta 150, 333-340
10. Rand,R.P. (1971) Biochim. Biophys. Acta 241, 823-834
11. Gulik-Krzywicki,T., Rivas,E. and Luzzati,V. (1967) J. Mol. Biol. 27, 303-322
12. Rand,R.P. and Luzzati,V. (1968) Biophys. J. 8, 125-137

13. Rivas,E. and Luzzati,V. (1969) J. Mol. Biol. 41, 261-275

14. Tardieu,A., Luzzati,V. and Reman,F.C. (1973) J. Mol. Biol. 75, 711-733

15. Ohshima,H. and Mitsui,T. (1978) J. Colloid Interface Sci.,in press

16. LeNeveu,D.M., Rand,R.P. and Parsegian,V.A. (1976) Nature 259, 601-603

17. LeNeveu,D.M., Rand,R.P., Parsegian,V.A. and Gingell, D. (1977) Biophys. J. 18, 209-230

18. Shipley,G.G., Leslie,R.B. and Chapman,D. (1969) Nature 222, 561-562

19. Shipley,G.G., Leslie,R.B. and Chapman,D. (1969) Biochim. Biophys. Acta 173, 1-10

20. Gulik-Krzywicki,T., Shechter,E., Luzzati,V. and Faure,M. (1969) Nature 223, 1116-1121

21. Butler,K.W., Hanson,A.W., Smith,I.C.P. and Schneider,H. (1973) Can. J. Biochem. 51, 980-989

22. Blaurock,A.E. (1973) Biophys. J. 13, 281-289

23. Sogor,B.V. and Zull,T.E. (1975) Biochim. Biophys. Acta 375, 363-380

24. Parsegian,V.A. (1966) Trans. Faraday Soc. 62, 848-860

25. Parsegian,V.A. (1967) J. Theoret. Biol. 15, 70-74

26. Parsegian,V.A. (1967) Science 156, 939-942

27. Gulik-Krzywicki,T., Luzzati,V. (1969) Mol. Cryst. Liq. Cryst. 8, 285-291

28. Palmer,K.J. and Schmitt,F.O. (1941) J. Cell Comp. Physiol. 17, 385-394

29. Gottlieb,M.H. and Eanes,E.D. (1972) Biophys. J. 12, 1533-1548

30. Shipley,G.G. (1973) in Biological Membranes (Chapman,D. and Wallach,D.F.H.,eds), Vol 2, p.23-25, Academic Press, London

31. Wilkins,M.H.F., Blaurock,A.E. and Engelman,D.M. (1971) Nat. New Biol. 230, 72-76

32. Furuya,K., Yamaguchi,T., Inoko,Y. and Mitsui,T. (1976) Acta Cryst. B32, 1811-1817

33. Shah,D.O. and Schulman,J.H. (1965) J. Lipid Res. 6, 341-349

34. Shah,D.O. and Schulman,J.H. (1967) J. Lipid Res. 8, 227-233

35. Seimiya,T. and Ohki,S. (1973) Biochim. Biophys. Acta 298, 546-561

36. Engelman,D.M. and Rothman,J.E. (1972) J. Biol. Chem. 247, 3694-3697

37. Dake,A., Finer,E.G., Flook,A.G. and Phillips,M.C. (1972) J. Mol. Biol. 63, 265-279

38. Phillips,M.C. and Finer,E.G. (1974) Biochim. Biophys. Acta 356, 199-206

39. Shimshick,E.J. and McConnell,H.M. (1973) Biochim. Biophys. Res. Commun. 53, 446-451

40. Shah,D.O. and Schulman,J.H. (1967) J. Lipid Res. 8, 215-226

41. Hinz,H.-J. and Sturtevant,J.M. (1972) J. Biol. Chem. 247, 6071-6075

42. Rand,R.P., Chapman,D. and Larsson,K. (1975) Biophys. J. 15, 1117-1124

43. Janiak,M.J., Small,D.M. and Shipley,G.G. (1976) Biochemistry 15, 4575-4580

44. Brady,G.W. and Fein,D.B. (1977) Biochim. Biophys. Acta 464, 249-259

45. Inoko,Y., yamaguchi,T., Furuya,K. and Mitsui,T. (1975) Biochim. Biophys. Acta 413, 24-32

46. Small,D.M. (1967) J. Lipid Res. 8, 551-557

47. Janiak,M.J., Loomis,C.R., Shipley,G.G. and Small,D.M. (1974) J. Mol. Biol. 86, 325-339

48. Untracht,S.H. and Shipley,G.G. (1977) J. Biol. Chem. 252, 4449-4457

49. Sheetz,M.P. and Chan,S.I. (1972) Biochemistry 11, 4573-4581

50. Handbook of Chemistry and Physics (1977) (Weast, R.C.,ed.), 57th ed., Section F, F-5, CRC Press Inc., Cleveland, Ohio

51. Hitchcock,P.B., Marson,R., Thomas,K.M. and Shipley, G.G. (1974) Proc. Nat. Acad. Sci. USA 71, 3036-3040

52. Salsbury,N.J., Darke,A. and Chapman,D. (1972) Chem. Phys. Lipids 8, 142-151

53. Furuya,K. and Mitsui,T., to be published

54. Mitsui,T. (1977) Advances in Biophys. 10, 178

55. Chapman,D., Peel,W.E., Kingston,B. and Lilley,T.H. (1977) Biochim. Biophys. Acta 464, 260-275

56. Shipley,G.G. (1973) in Biological Membranes (Chapman, D. and Wallach,D.F.H.,eds), Vol.2, p.43-48, Academic Press, London

57. Spartz,L. and Strittmatter,P. (1971) Proc. Nat. Acad. Sci. USA 68, 1042-1046

58. Dufourcq,J., Bernon,R. and Lussan,C. (1976) Biochim. Biophys. Acta 433, 252-263

59. Lowry,O.H., Rosebrough,N.J., Fau,A.L. and Randalli, R.J. (1951) J. Biol. Chem. 193, 265-275

60. Andrews,P. (1964) Biochem. J. 91, 222-233

61. Inoko,Y. and Mitsui,T. (1978) to be submitted to J. Phys. Sco. Japan

62. Visser,V., Robinson,N.C. and Tanford,C. (1975) Biochemistry 14, 1194-1199

63. Luzzati,V., Witz,J. and Nicolaieff,A. (1961) J. Mol. Biol. 3, 379-392

64. Bloomfield,V. (1966) Biochemistry 5, 684-689

65. Mathews,F.S. and Strittmatter,P. (1969) J. Mol. Biol. 41, 295-297

66. Ito,A. and Sato,R. (1968) J. Biol. Chem. 243, 4922-4930

67. Calabro,M.A., Katz,J.T. and Holloway,P.W. (1976) J. Biol. Chem. 251, 2113-2118

68. Faucon,J.-F., Dufourcq,J., Lussan,C. and Bernon,R. (1976) Biochim. Biophys. Acta 436, 283-294

69. Bolduan,O.E.A. and Bear,R.S. (1949) J. Appl. Phys. 20, 983-992

70. Franks,A. (1955) Proc. Phys. Soc. B68, 1054-1064

71. Franks,A. (1958) Brit. J. Appl. Phys. 9, 349

72. Elliott,A. (1965) J. Sci. Instrum. 42, 312-316

73. Bragg,W.L. and Perutz,M.F. (1952) Proc. Roy. Soc. Ser A 213, 425

74. Torbet,J. and Wilkins,M.H.F. (1976) J. Theor. Biol. 62, 447-458

75. Lesslauer,W., Cain,J.E. and Blasie J.K.(1971) Biochim. Biophys. Acta 241, 547-566

76. Lesslauer,W., Cain,J.E. and Blasie,J.K. (1972) Proc. Nat. Acad. Sci. USA 69, 1499-1503